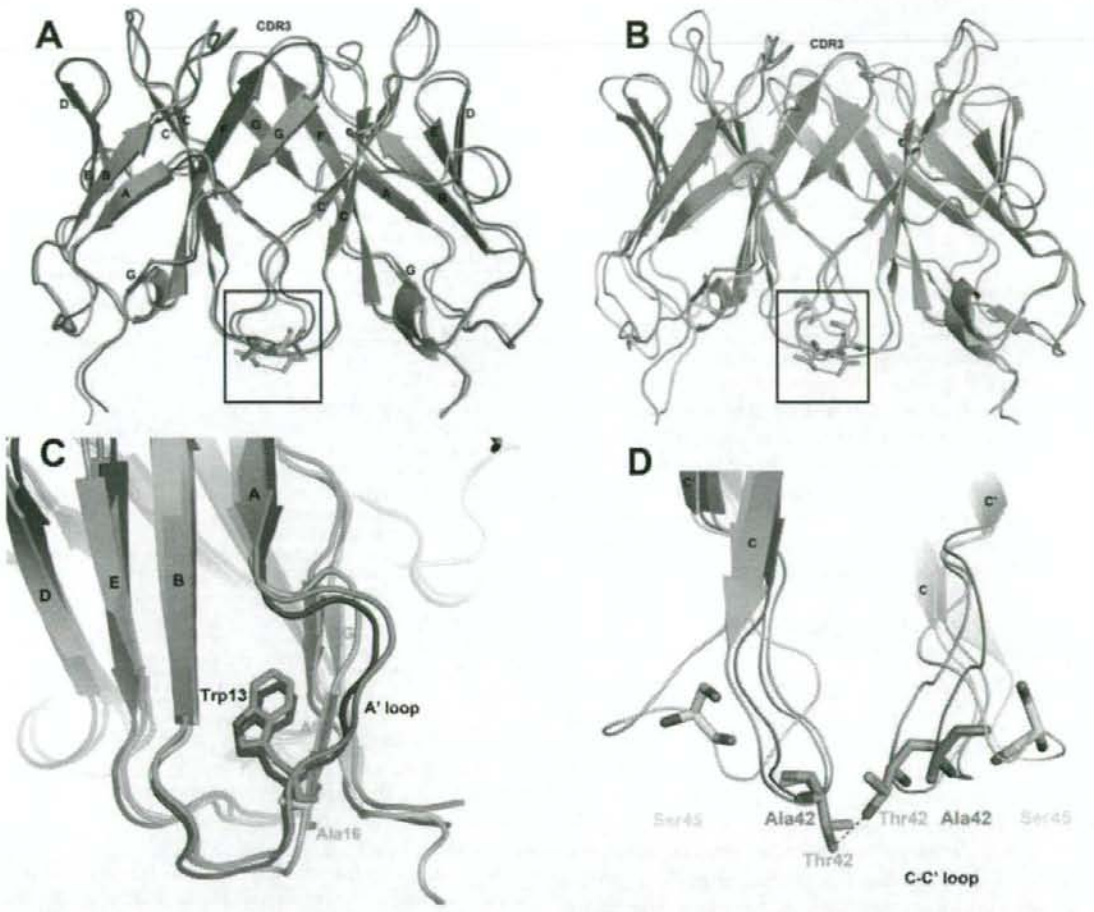


**Figure 1**

Crystal structure of rCD8αα homodimer and its superposition with human and mouse CD8αα structures. The ribbon diagram of each CD8αα was drawn and color-coded as: rCD8αα, green and cyan; hCD8αα, blue and magenta; mCD8αα, yellow and orange. (**A**) Superposition of rCD8αα and hCD8αα. The extra hydrogen bond region of rCD8αα was boxed. (**B**) Superposition of rCD8αα and mCD8αα. The extra hydrogen bond region of rCD8αα was boxed. (**C**) The transition of A'-β strand in mCD8αα and A' loop in both rCD8αα/hCD8αα as the residue changes (Ala16 to Trp13). (**D**) Thr43 residues in C-C' loop of rCD8αα homodimer (cyan) form extra hydrogen bonds. Hydrogen bond between two main-chains is shown as red dashed line.

determining regions (CDRs), which are involved in MHCIs binding. Interestingly, though CDR1 and CDR2 are structurally variable, CDR3 has almost the same conformation among r/h/m CD8αα molecules [Fig. 1(A,B)].

As one of the elements commonly found in many Ig domains, the first β strand of each domain is split into two shorter strands (A and A′).[20] rCD8αα homodimer can also be characterized by a *cis*-proline (Pro7) at the transition point at the A strand. However, at the place of the A′ strand, a loop is located in rhesus macaque as well as human CD8α molecules as the result of the big side chain of the residue Trp13, which is equivalent to Ala16 in mCD8α molecules [Fig. 1(C)].

Corresponding to Ala42 in hCD8α and Ser48 in mCD8α, Thr43 residues in rCD8α form an additional hydrogen bond to each other. This extra H-bond enhances the dimeric interaction and brings the C–C′ loop of the two molecules into a much closer position [Fig. 1(D)]. As a result, the interface size of the two rCD8α subunits (~2274 Å$^2$, total buried solvent-accessible surface area) is significantly larger than that of human CD8α interface (~2038 Å$^2$) indicating a tighter homodimeric interaction of CD8αα in rhesus macaque.

## ACKNOWLEDGMENTS

The authors thank Dr. Fuliang Chu for his valuable suggestions for this project and Mr. Christopher Pannell for his critical reading of the manuscript.

## REFERENCES

1. Allen TM, Sidney J, del Guercio MF, Glickman RL, Lensmeyer GL, Wiebe DA, DeMars R, Pauza CD, Johnson RP, Sette A, Watkins DI. Characterization of the peptide binding motif of a rhesus MHC class I molecule (Mamu-A*01) that binds an immunodominant CTL epitope from simian immunodeficiency virus. J Immunol 1998;160:6062–6071.
2. Matano T, Shibata R, Siemon C, Connors M, Lane HC, Martin MA. Administration of an anti-CD8 monoclonal antibody interferes with the clearance of chimeric simian/human immunodeficiency virus during primary infections of rhesus macaques. J Virol 1998;72:164–169.
3. Schmitz JE, Kuroda MJ, Santra S, Sasseville VG, Simon MA, Lifton MA, Racz P, Tenner-Racz K, Dalesandro M, Scallon BJ, Ghrayeb J, Forman MA, Montefiori DC, Rieber EP, Letvin NL, Reimann KA. Control of viremia in simian immunodeficiency virus infection by CD8+ lymphocytes. Science 1999;283:857–860.
4. Kaufmann SH, McMichael AJ. Annulling a dangerous liaison: vaccination strategies against AIDS and tuberculosis. Nat Med 2005;11: S33–S44.
5. Fung-Leung WP, Schilham MW, Rahemtulla A, Kundig TM, Vollenweider M, Potter J, van Ewijk W, Mak TW. CD8 is needed for development of cytotoxic T cells but not helper T cells. Cell 1991;65:443–449.
6. Cole DK, Gao GF. CD8: adhesion molecule, co-receptor and immuno-modulator. Cell Mol Immunol 2004;1:81–88.
7. Leishman AJ, Naidenko OV, Attinger A, Koning F, Lena CJ, Xiong Y, Chang HC, Reinherz E, Kronenberg M, Cheroutre H. T cell responses modulated through interaction between CD8αα and the nonclassical MHC class I molecule, TL. Science 2001;294:1936–1939.
8. Wyer JR, Willcox BE, Gao GF, Gerth UC, Davis SJ, Bell JI, van der Merwe PA, Jakobsen BK. T cell receptor and coreceptor CD8 αα bind peptide-MHC independently and with distinct kinetics. Immunity 1999;10:219–225.
9. Cole DK, Rizkallah PJ, Boulter JM, Sami M, Vuidepot AL, Glick M, Gao F, Bell JI, Jakobsen BK, Gao GF. Computational design and crystal structure of an enhanced affinity mutant human CD8 αα coreceptor. Proteins 2007;67:65–74.
10. Sewell AK, Gerth UC, Price DA, Purbhoo MA, Boulter JM, Gao GF, Bell JI, Phillips RE, Jakobsen BK. Antagonism of cytotoxic T-lymphocyte activation by soluble CD8. Nat Med 1999;5:399–404.
11. Gao GF, Jakobsen BK. Molecular interactions of coreceptor CD8 and MHC class I: the molecular basis for functional coordination with the T-cell receptor. Immunol Today 2000;21:630–636.
12. Gao GF, Rao Z, Bell JI. Molecular coordination of αβ T-cell receptors and coreceptors CD8 and CD4 in their recognition of peptide-MHC ligands. Trends Immunol 2002;23:408–413.
13. Gao GF, Gerth UC, Wyer JR, Willcox BE, O'Callaghan CA, Zhang Z, Jones EY, Bell JI, Jakobsen BK. Assembly and crystallization of the complex between the human T cell coreceptor CD8α homodimer and HLA-A2. Protein Sci 1998;7:1245–1249.
14. Gao GF, Tormo J, Gerth UC, Wyer JR, McMichael AJ, Stuart DI, Bell JI, Jones EY, Jakobsen BK. Crystal structure of the complex between human CD8α(α) and HLA-A2. Nature 1997;387:630–634.
15. Kern PS, Teng MK, Smolyar A, Liu JH, Liu J, Hussey RE, Spoerl R, Chang HC, Reinherz EL, Wang JH. Structural basis of CD8 coreceptor function revealed by crystallographic analysis of a murine CD8αα ectodomain fragment in complex with H-2Kb. Immunity 1998;9:519–530.
16. Liu Y, Xiong Y, Naidenko OV, Liu JH, Zhang R, Joachimiak A, Kronenberg M, Cheroutre H, Reinherz EL, Wang JH. The crystal structure of a TL/CD8αα complex at 2.1 A resolution: implications for modulation of T cell activation and memory. Immunity 2003;18:205–215.
17. Chang HC, Tan K, Ouyang J, Parisini E, Liu JH, Le Y, Wang X, Reinherz EL, Wang JH. Structural and mutational analyses of a CD8αβ heterodimer and comparison with the CD8αα homodimer. Immunity 2005;23:661–671.
18. Chu F, Lou Z, Chen YW, Liu Y, Gao B, Zong L, Khan AH, Bell JI, Rao Z, Gao GF. First glimpse of the peptide presentation by rhesus macaque MHC class I: crystal structures of Mamu-A*01 complexed with two immunogenic SIV epitopes and insights into CTL escape. J Immunol 2007;178:944–952.
19. Otwinowski Z, Minor W. Processing of X-ray diffraction data collected in oscillation mode. Methods Enzymol 1997;276:307–326.
20. Chen Y, Chu F, Gao F, Zhou B, Gao GF. Stability engineering, biophysical, and biological characterization of the myeloid activating receptor immunoglobulin-like transcript 1 (ILT1/LIR-7/LILRA2). Protein Expr Purif 2007;56:253–260.
21. CCP4. The CCP4 suite: programs for protein crystallography. Acta Crystallogr D Biol Crystallogr 1994;50:760–763.
22. Lovell SC, Davis IW, Arendall WB, III, de Bakker PI, Word JM, Prisant MG, Richardson JS, Richardson DC. Structure validation by Cα geometry: π,ψ and Cβ deviation. Proteins 2003;50:437–450.
23. Gao GF, Willcox BE, Wyer JR, Boulter JM, O'Callaghan CA, Maenaka K, Stuart DI, Jones EY, Van Der Merwe PA, Bell JI, Jakobsen BK. Classical and nonclassical class I major histocompatibility complex molecules exhibit subtle conformational differences that affect binding to CD8αα. J Biol Chem 2000;275:15232–15238.

Analytical Biochemistry 385 (2009) 278–285

Contents lists available at ScienceDirect

Analytical Biochemistry

journal homepage: www.elsevier.com/locate/yabio

# *Thermus thermophilus*-derived protein tags that aid in preparation of insoluble viral proteins

Naoyuki Kondo [a,b], Akio Ebihara [c,1], Heng Ru [b], Seiki Kuramitsu [c,d], Aikichi Iwamoto [a,e], Zihe Rao [b,f], Zene Matsuda [a,b,*]

[a] Research Center for Asian Infectious Diseases, Institute of Medical Science, University of Tokyo, 4-6-1, Shirokanedai, Minato-ku, Tokyo 108-8639, Japan
[b] China–Japan Joint Laboratory of Structural Virology and Immunology, Institute of Biophysics, Chinese Academy of Sciences, Beijing 100101, People's Republic of China
[c] RIKEN SPring-8 Center, Harima Institute, Hyogo 679-5148, Japan
[d] Department of Biological Sciences, Graduate School of Science, Osaka University, Osaka 560-0043, Japan
[e] Division of Infectious Diseases, Advanced Clinical Research Center, Institute of Medical Science, University of Tokyo, Tokyo 108-8639, Japan
[f] National Laboratory of Biomacromolecules, Institute of Biophysics, Chinese Academy of Sciences, Beijing 100101, People's Republic of China

ARTICLE INFO

*Article history:*
Received 1 September 2008
Available online 19 November 2008

*Keywords:*
*Thermus thermophilus*
HIV
Protein tag
Solubilization
Vpr
Membrane-spanning domain

ABSTRACT

The expression and solubilization of insoluble proteins have been facilitated by the introduction of protein tags. In our analyses of viral protein R (Vpr) of human immunodeficiency virus 1 (HIV-1), however, several conventional tag proteins enhanced its expression but failed to solubilize it. Therefore, we decided to explore whether proteins derived from *Thermus thermophilus* HB8 (*T. th.*), a highly heat-stable bacterium, could be used as tag proteins to enhance the solubilization of Vpr. Based on the data accumulated during the recent structural genomics project of *T. th.*, we selected 15 *T. th.* proteins with high expression levels and solubilities. From this group, we identified a *T. th.* tag protein that expressed Vpr in a soluble form. Furthermore, two *T. th.* tag proteins, including the identified one, were found to solubilize the extremely insoluble membrane-spanning domain of the envelope protein of HIV-1. When green fluorescent protein (GFP) was used as a passenger protein of *T. th.* tags, the brightness and stability of GFP were similar to those of untagged GFP, suggesting that the *T. th.* tags do not negatively affect the function of the passenger protein. Thus, data of structural genomics can be applied to generate a customized versatile protein tag for protein analyses.



The structures of various proteins have been determined during recent years, owing mainly to the progress of structural genomics (SG)[2] research. This information not only enriches our knowledge of certain aspects of basic protein science, such as protein-folding patterns and specific protein–protein interactions, but also provides practical contributions for structure-oriented drug design against pathogens [1–5]. The structures of some proteins remain unknown, however, because the proteins have unfavorable properties that hinder attempts to analyze their structures. Such properties include low expression level, low solubility, difficulty of purification, poor crystallizability, and instability of formed crystals. Adaptor proteins that interact with multiple other proteins, or membrane proteins with highly hydrophobic segments, often possess these properties.

The use of certain tag proteins can overcome some of these problems. A small peptide tag such as a polyhistidine tag, for example, can facilitate both the detection and purification of a target protein [6,7]. Some larger peptide tags (or protein tags) can likewise improve detection and purification while also enhancing the expression level and solubility of a protein of interest. Indeed, maltose binding protein (MBP) [8], glutathione *S*-transferase (GST) [9], thioredoxin (TRX) [10], and N utilization substance A (NusA) [11] have been widely used, and several expression vectors are commercially available. Several groups have compared the efficiency of conventional tag proteins for expression [12–15]. Although each of these studies used different expression vectors and passenger proteins, it seems reasonable to conclude that one should try several tag proteins for a particular passenger protein because the potency of a tag can be affected by multiple factors,

* Corresponding author. Address: Research Center for Asian Infectious Diseases, Institute of Medical Science, University of Tokyo, 4-6-1, Shirokanedai, Minato-ku, Tokyo 108-8639, Japan. Fax: +81 3 6409 2208.
*E-mail address:* zmatsuda@ims.u-tokyo.ac.jp (Z. Matsuda).
[1] Present address: Laboratory of Applied Biochemistry, Faculty of Applied Biological Sciences, Gifu University, Gifu 501-1193, Japan.

[2] *Abbreviations used:* SG, structural genomics; MBP, maltose binding protein; GST, glutathione *S*-transferase; TRX, thioredoxin; NusA, N utilization substance A; HIV, human immunodeficiency virus; SIV, simian immunodeficiency virus; AIDS, acquired immunodeficiency syndrome; Vpr, virus protein R; MSD, membrane-spanning domain; *T. th.*, *Thermus thermophilus*; GFP, green fluorescent protein; Vpx, viral protein X; PCR, polymerase chain reaction; LB, Luria–Bertani; IPTG, isopropylthiogalactoside; SDS–PAGE, sodium dodecyl sulfate–polyacrylamide gel electrophoresis; PBS, phosphate-buffered saline; GdmHCl, guanidium hydrochloride; CD, circular dichroism; UV, ultraviolet; FACS, fluorescence-activated cell sorting.

0003-2697/$ - see front matter © 2008 Elsevier Inc. All rights reserved.
doi:10.1016/j.ab.2008.10.050

including the specific properties of the passenger proteins as well as the linker between the tag and passenger proteins.

In many cases, tag proteins serve as molecular chaperons during the synthesis and folding of the passenger protein [12], only to be removed after production and purification. For an extremely insoluble passenger protein, a tag protein is retained so as to facilitate solubilization. If a proper tag protein is selected, the passenger protein's function is well maintained even with a fused tag form [16]. Moreover, the remaining tag proteins, if their structures are known, can serve as models of molecular replacement for phase determination [16,17]. Lysozyme [18], MBP [19], and GST [20] have been successfully used for this purpose.

In our laboratory, we are studying the several proteins of primate lentiviruses, human immunodeficiency virus (HIV), and simian immunodeficiency virus (SIV) that are linked with acquired immunodeficiency syndrome (AIDS). One of them is virus protein R (Vpr), and another is gp41, a subunit of envelope protein. Vpr is a highly insoluble 14-kDa accessory gene product of HIV-1. It works as a pleiotropic adaptor protein in the life cycle of HIV-1 [21–26]. The gp41 subunit plays a critical role for membrane fusion and contains highly hydrophobic membrane-spanning domain (MSD). The membrane-spanning domain of gp41 (gp41-MSD) anchors the HIV-1 envelope protein to lipid bilayers [27]. During our study of these insoluble proteins, we tried to improve solubilization by using several conventional tag proteins but had limited success. Therefore, we tried to identify new tag proteins that would facilitate the production and structure determination of proteins of interest. We sought candidate tag proteins from *Thermus thermophilus* (*T. th.*), one of the well-characterized model organisms of the SG project [28,29]. Because *T. th.* survives at 85 °C and its proteins are heat-stable [30], the structures of more than 400 of approximately 2000 known gene products have been determined during the past 5 years [28]. Drawing on information that has accumulated from SG research on *T. th.* proteins, we tested proteins with high expression and solubility characteristics and known high-resolution three-dimensional structures for their utility as candidate tag proteins.

We tested 15 candidate tag proteins on Vpr of HIV-1 and identified a *T. th.* tag protein that could express a soluble form of Vpr. This tag and another tag were also able to help expression of a gp41-MSD. Analyses using green fluorescent protein (GFP) as a fusion passenger protein suggested that these *T. th.* tags did not significantly affect the biophysical properties of the passenger proteins. Our results suggest that the information accumulated during the SG project, as exemplified here for *T. th.*, can be a versatile resource for the identification of customized tag proteins that may facilitate biophysical and structural analyses of highly insoluble proteins.

## Materials and methods

### *Selection of candidate tag proteins from T. th*

We used the accumulated data from expression, purification, and crystallization trials in the Whole Cell Project of *T. th.* [29,31] to select candidate proteins. From the more than 400 proteins with known structures, we selected proteins that showed good expression and solubility. In the Whole Cell Project of *T. th.*, we arbitrarily defined seven classes to indicate a protein's expression level and solubility fitness: (i) no expression, (ii) low expression and low solubility, (iii) high expression and low solubility, (iv) high expression and half solubility, (v) low expression and high solubility, (vi) high expression and half solubility, and (vii) high expression and high solubility. We selected proteins that fell in the high expression and high solubility category. Among these selected proteins, we further narrowed the field by choosing candidates whose resolution of the determined structure is higher than 2 Å.

### *Construction of expression plasmids*

All of the proteins were expressed in *Escherichia coli* BL21 Star (DE3) (Invitrogen) using the same plasmid derived from pET-47b (Novagen). pET-47b contains a T7 promoter, a six polyhistidine tag-coding sequence, and an HRV 3C protease recognition sequence upstream of the multiple cloning site. A tag protein was added at either the N or C terminus of a passenger protein (Fig. 1). To add the tag at the N terminus, we used a modified pET-47b plasmid called pET-47md that had been produced by cloning an oligonucleotide cassette with *Asc*I, *Pac*I, *Bam*HI, and *Bsr*GI sites, in that order, between the *Kpn*I and *Avr*II sites of pET-47b. To fuse a candidate tag protein at the C terminus of a passenger protein, pET-47b was used. The pET-47b vector has *Bam*HI, *Bsr*GI, *Asc*I, and *Pac*I sites, in that order, in the multiple cloning site.

The genes for tag proteins were amplified by polymerase chain reaction (PCR) using primers that contained *Asc*I and *Pac*I sites at the 5′ and 3′ termini of the genes while also using KOD Plus (Toyobo), Pfu Turbo (Stratagene), and Ex Taq (Takara) DNA polymerases. The template DNAs we used included 15 *T. th.* expression plasmids for *T. th.* genes [31,32] (RIKEN Bioresource Center DNA bank), pMALp2e (New England Biolabs) for *mbp*, pGEX5x-1 (GE Healthcare) for *gst*, pET-50b (Novagen) for *nusA*, pSP65HXB2gpt for *vpr*, and the synthetic *vpx* (viral protein X) gene whose sequence is based on that of SIVmac251 and optimized for yeast codon use. Modified GFPs, which were used as passenger proteins, were also amplified by PCR using primers with *Bam*HI and *Bsr*GI sites at the 5′ and 3′ termini, respectively [33]. The MSD portion of gp41 [27] was synthesized as a complementary pair of oligode-

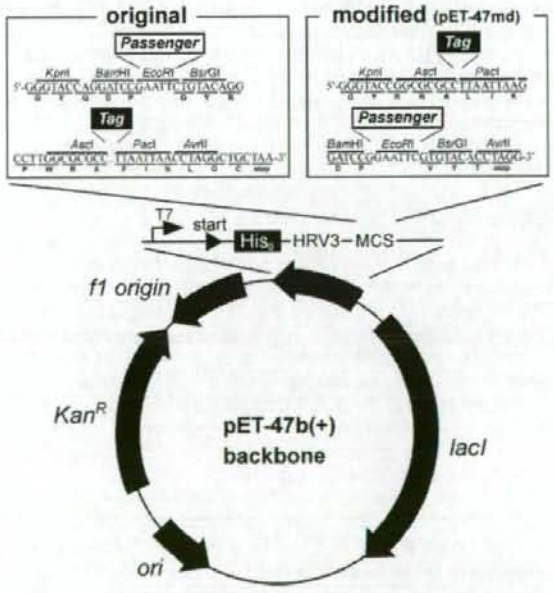


**Fig. 1.** Schematic representation of plasmids used in this study. The upper panel shows the details of the multiple cloning site of pET-47b and pET-47md. The lower panel shows the structure of the backbone. T7, T7 promoter; $His_6$, polyhistidine tag; HRV3, region coding amino acid sequences recognized by HRV 3C protease; MCS, multiple cloning site; Tag, genes of tag proteins; Passenger, genes of passenger proteins.

oxyribonucleotides with *Bam*HI and *Bsr*GI sites at the 5′ and 3′ termini, respectively. All amplicons were first cloned into pCR4blunt-TOPO vectors using the TOPO Cloning Kit (Invitrogen), and their sequences were verified before being cloning into pET-47b or pET-47md. After cloning the individual passenger gene between the *Bam*HI and *Bsr*GI sites of pET-47b or pET-47md, the respective tag genes were cloned using the *Asc*I and *Pac*I sites. As a control, we constructed expression vectors containing tag genes but without passenger genes; this was accomplished by cloning the tag genes to pET-47md with the *Asc*I and *Pac*I sites. We verified all sequences of the constructed expression vectors.

*Analysis of protein expression on a small-scale*

BL21 Star (DE3) (Invitrogen) was transformed by the constructed expression plasmids and cultured on Luria–Bertani (LB) plates containing 50 μg/ml kanamycin. Fresh colonies were picked and inoculated into 2 ml of LB medium containing 50 μg/ml kanamycin. All *E. coli* cells were grown at 37 °C throughout the experiments. When the cells had reached a log phase, isopropylthiogalactoside (IPTG) was added in a final concentration of 1 mM. After a 5-h growth period, the cells were harvested by centrifuging at 15,000g for 10 min at 4 °C using an MX-301 centrifuge (Tomy). We extracted the expressed proteins using 300 μl of BugBuster (Novagen) that contained 0.3 μl of Benzonase (Novagen). The total lysate and supernatant was subjected to sodium dodecyl sulfate–polyacrylamide gel electrophoresis (SDS–PAGE) using a 5% to 20% SDS gradient gel (DRC). We confirmed the expressed protein with the peptide mass fingerprinting method using AXIMA-CFR Plus (Shimadzu).

*Measurement of fluorescent activity of GFP*

BL21 Star (DE3) cells that had been transformed using the GFP expression vectors (GFP alone or tag-fused GFP at the N terminus) were grown for 5 h in LB medium containing 1 mM IPTG and then harvested by centrifugation (15,000g, 4 °C). The cell pellets were suspended in 0.7 ml of phosphate-buffered saline (PBS), and the optical densities at 600 nm were determined. The fluorescence of the suspended cells was analyzed using a FACSCalibur flow cytometer (BD Biosciences). We normalized the measured mean fluorescence signal by dividing it by the obtained optical densities at 600 nm ($OD_{600}$).

*Analysis of stability of tagged protein*

A 20-μl aliquot of the supernatant of tag-free or tag-fused GFP-expressing cell lysate prepared as described above was added to a 500-μl buffer solution containing 20 mM Tris–HCl (pH 8.0) and increasing concentrations (1, 2, 3, 4, and 5 M) of guanidium hydrochloride (GdmHCl). After incubating the preparations for 1 day at room temperature, we measured the emission spectra from 500 to 600 nm using an F-4500 fluorescence spectrophotometer (Hitachi) set to an excitation wavelength of 470 nm.

*Large-scale expression and purification*

BL21 Star (DE3) cells transformed with individual expression plasmids were grown in 1 L of LB medium containing 50 μg/ml kanamycin. When $OD_{600}$ reached 0.5 to 0.7, IPTG was added to produce a final concentration of 1 mM so as to induce the expression of target proteins. After a 5-h growth period, cells were pelleted down and frozen at −30 °C. To extract the protein, the cell pellets were resuspended in buffer A (20 mM NaPi [pH 7.4], 0.5 M NaCl, and 20 mM imidazole). The suspended cells were placed on ice and subjected to ultrasonication for 1 h. The disrupted cell extract was centrifuged at 5000g for 30 min at 4 °C to remove insoluble materials. The supernatants were loaded onto Ni Sepharose 6 Fast Flow columns (GE Healthcare) and eluted with a second buffer (20 mM NaPi [pH 7.4], 0.5 M NaCl, and 0.5 M imidazole). HRV 3 C protease (Novagen) was added to the eluted fractions, and the preparations were incubated at 4 °C for more than 16 h to remove the polyhistidine tags. After exchanging the second buffer for buffer A using VivaSpin (Sartorius), the solutions again were loaded onto Ni Sepharose 6 Fast Flow columns. The flow-through fraction was collected and concentrated to 2 to 5 ml in a buffer containing 50 mM Tris–HCl (pH 8.0) and 0.5 M NaCl. The concentrated fraction was subjected to Superdex 200 size exclusion chromatography using an AKTA Purifier (GE Healthcare). We collected the highest peaks and verified their content using SDS–PAGE.

*Secondary structure analyses*

Purified proteins were placed in buffer (20 mM NaPi [pH 7.0] and 0.5 M NaCl), and their circular dichroism (CD) in the far-UV (ultraviolet) region of 200 to 250 nm was measured at 25 °C using a Pistar-180 Spectrometer (Applied Photophysics).

## Results

*Expression of Vpr protein with conventional tag fusion*

To obtain soluble Vpr protein for future analysis, we tried to express Vpr in *E. coli*. When Vpr was expressed without any tag, it did not express very well. Even when it was expressed, it did not come to a soluble fraction (Fig. 2A). This is consistent with previous studies [26,34]. The conventional tag genes *mbp*, *gst*, and *nusA* were introduced upstream or downstream of the HIV *vpr* gene in the expression plasmid (Fig. 1). Among the conventional tag proteins, GST and NusA facilitated expression of fusion protein when added at the N or C terminus, whereas MBP failed to achieve a high expression level (Fig. 2B). Unfortunately, all of the tagged Vpr proteins that were expressed were observed in the insoluble fraction (Fig. 2B).

*Selection of candidate T. th. tag protein*

To seek other effective tags for Vpr protein expression and solubilization, we decided to introduce proteins from *T. th.*; the SG project of *T. th.* [28] has provided many data sets, including those for protein expression, purification, and crystallization [29], that aided in our selection of viable candidates for this effort. We selected 59 candidates from more than 400 proteins based on their expression level and the solubility (see Materials and methods for details). From these 59, we selected 31 candidates with resolutions of structures higher than 2 Å. By coincidence, the molecular weight of each of the 31 candidates was less than 40 kDa. This may reflect the fact that smaller molecular weight proteins are easier to express and crystallize [35].

We further narrowed the candidate pool by selecting 14 proteins for which information on small-scale protein preparation was available. To these 14 candidates, we added a 57.9-kDa protein, the largest in the first-pass group of 59 proteins. We included this protein so as to have a larger molecular weight tag protein that could serve as a favorable model of molecular replacement for larger passenger proteins. The complete list of 15 candidate proteins appears in Table 1. As a group, there seemed to be no common functional or structural correlations, probably because we selected the candidates solely for their practical properties of expression and solubility and on their structural analyses.

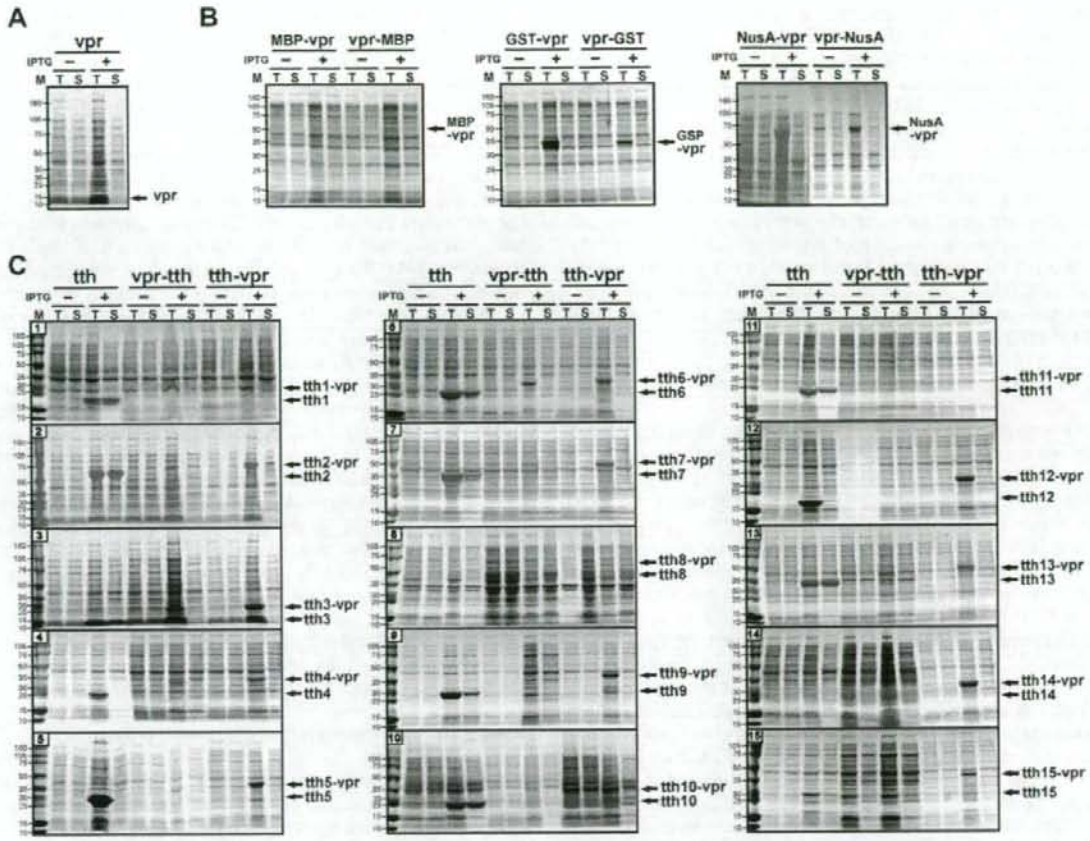


**Fig. 2.** Expression profile of tag protein-fused Vpr with (+) or without (−) induction by IPTG. Based on calculated molecular weights, the positions of expected proteins are marked by arrows along the right edge of each gel. (A) Expression profiles of tag-free Vpr. (B) Expression profiles of MBP-fused Vpr, GST-fused Vpr, and NusA-fused Vpr. (C) Expression profiles of individual *T. th.* protein candidates alone (tth) and when fused with Vpr at the C terminus (vpr–tth) or at the N terminus (tth–vpr). The number indicated in the box in the upper left corner of each gel corresponds to the number used for the candidate tth gene listed in Table 1. Gel columns indicate molecular weight markers (in kDa) (M), total lysate (T), and supernatant (S).

**Table 1**
Selected candidates of protein tags from *T. th.*

| Name in this study | Locus tag in genome | Functional feature | $M_W$ (kDa) | PDB ID | Resolution (Å) |
|---|---|---|---|---|---|
| tth1 | TTHA0132 | Conserved hypothetical protein | 16.9 | 2dx6 | 1.78 |
| tth2 | TTHA0271 | Molecular chaperon, GroEL | 57.9 | 1wf4 | 2.80 |
| tth3 | TTHA0281 | UPF0150 family protein | 9.8 | 2dsy | 1.90 |
| tth4 | TTHA0341 | Molybdopterin biosynthesis enzyme MoaB | 17.8 | 2is8 | 1.64 |
| tth5 | TTHA1053 | Conserved hypothetical protein | 20.7 | 2cve | 1.60 |
| tth6 | TTHA1091 | Conserved hypothetical protein | 17.8 | 1vgg | 1.75 |
| tth7 | TTHA1199 | Ornithine carbamoyltransferase | 33.3 | 2ef0 | 2.00 |
| tth8 | TTHA1275 | C subunit of $V_1 - V_0$ ATPase | 36.0 | 1v9m | 1.85 |
| tth9 | TTHA1359 | Transcriptional regulator | 22.4 | 2zcw | 1.50 |
| tth10 | TTHA1671 | Adenylate kinase | 20.7 | 3cm0 | 1.80 |
| tth11 | TTHA1699 | Putative transediting enzyme of tRNA-Syn | 16.6 | 2cx5 | 1.90 |
| tth12 | TTHA1713 | Conserved hypothetical protein | 14.4 | 2cu5 | 1.84 |
| tth13 | TTHA1838 | Atypical ABC-ATPase, SufC | 27.6 | 2d2f | 1.90 |
| tth14 | TTHA1897 | GidA-related protein | 25.9 | 2cul | 1.65 |
| tth15 | TTHB192 | CRISPR-associated protein | 23.8 | 1wj9 | 1.90 |

*Expression of Vpr protein with T. th. protein fusion*

Because the expression vectors used in this study (pET-47b and pET-47md) (Fig. 1) have the polyhistidine and protease recognition sequences that are absent from the vectors used in the *T. th.* SG project (pET-3a and pET-11a) [28,29], we began our investigation by evaluating the selected *T. th.* proteins in the pET-47b backbone. Our results showed that although all *T. th.* proteins were expressed well, 7 of the 15 *T. th.* proteins (Tth4, Tth5, Tth7, Tth8, Tth12, Tth14, and Tth15) failed to solubilize (Fig. 2C, tth). Because the general

conditions for the expression, such as growth medium, growth temperature (37 °C), and IPTG concentration, were identical to those of the original *T. th.* SG project, the differences in the used expression vectors, especially the presence of a polyhistidine tag and the protease recognition site in the pET-47md backbone, seem to have affected the solubility of the *T. th.* proteins.

Then we tested the expression level and the solubility of *T. th.* tag-fused Vpr. Except for tags Tth1, Tth8, and Tth11, all *T. th.* tags facilitate the expression level of the fusion protein when the *T. th.* proteins had been added at the N terminus of Vpr (Fig. 2C, tth–vpr). However, in the case of C terminus addition, only the Tth6-fused protein among the *T. th.* tag-fused Vpr proteins was expressed well (Fig. 2C, vpr–tth).We found that the Tth2 protein enhanced the solubility of Vpr when Tth2 was added to the N terminus of Vpr (Fig. 2C).

*Efficacy of the tag proteins on other insoluble proteins*

We investigated the efficacy of *T. th.* tag proteins on other insoluble proteins from primate lentiviruses. Based on the results of *T. th.* alone or *T. th.* in a Vpr fusion form (Fig. 2), seven *T. th.* tags (Tth2, Tth3, Tth6, Tth9, Tth10, Tth11, and Tth13) were introduced to the N terminus of two lentiviral proteins. Three conventional tags were also introduced to this position. One of these proteins, gp41-MSD, is a highly hydrophobic 2.2-kDa peptide that anchors the envelope protein to lipid bilayers [27]. The synthetic peptide of gp41-MSD remains insoluble under the condition of 100% dimethyl sulfoxide (unpublished data). Another protein, Vpx, is a virion-associated 12.9-kDa protein of SIV that plays an important role in nuclear transport of the incoming preintegration complex [26]. Vpr and Vpx are evolutionarily related to each other and have approximately 15% of their primary structures in common. Among the conventional tags, MBP and NusA enhanced the expression level of tag-fused gp41-MSD (Fig. 3A), but the expressed proteins could not be found in the soluble fractions (Fig. 3A). Six *T. th.* tags (Tth2, Tth6, Tth9, Tth10, Tth11, and Tth13) enhanced expression levels when fused at the N terminus (Fig. 3B). Both the Tth2 and Tth10 proteins were partially successful at solubilizing gp41-MSD (Fig. 3B). In the case of Vpx, expression levels were enhanced when fused with NusA, Tth2, Tth3, Tth6, Tth9, Tth10, Tth11, and Tth13, although none of these fusion proteins could be solubilized (data not shown). These results suggest that *T. th.*-tagged proteins can enhance the expression level of insoluble proteins; however, the efficacy depends heavily on the passenger proteins used.

*Effect of tag proteins on the function of passenger proteins*

It is of interest to know whether fusion of a tag may affect any functions of the fused passenger protein. We attempted to test what effect, if any, the *T. th.* tag-fused Vpr had on the cell cycle, but our efforts at transduction of the purified proteins into the mammalian cells were not too successful. In the case of gp41-MSD, there is no good biological assay because it is a portion of a protein. Therefore, we used GFP as a surrogate reporter for Tth2, Tth6, Tth9, Tth10, Tth11, and Tth13. Most of the tag proteins, such as Tth2, Tth3, Tth6, and Tth9, enhanced expression to levels comparable to those achieved with the conventional tags GST and NusA (Fig. 4A). Moreover, Tth2, Tth10, and Tth13 proteins enhanced the solubility of fused GFPs. The fluorescence-activated cell sorting (FACS) analyses of the fluorescence of the fused GFPs showed that the fluorescent intensity of MBP, GST, Tth11, and Tth13 fused proteins was less than half the intensity of intact GFP (Fig. 4B). As shown in Fig. 4A, both the expression level and solubility of these fusion proteins were similar to those of intact GFP; however, the fusion with these tags reduced the activity of GFP. In the case of Tth2, Tth3, Tth6, Tth9, and Tth10 proteins, the fusion affected the fluorescence of GFP only slightly.

We next examined the stability of the tagged GFPs under denaturing conditions by treating the proteins with GdmHCl (Fig. 4C and D). For the conventional tag proteins, the denaturation profile of GST-fused GFP was nearly identical to that of intact GFP, although for MBP and NusA the normalized fluorescence intensities of the tag-fused proteins were slightly lower than the intensity of intact GFP (Fig. 4C). On the other hand, all denaturation profiles of *T. th.* tag-fused proteins, except for Tth13, were similar to the profile of tag-free GFP (Fig. 4D). These results suggest that the *T. th.* tag proteins do not destabilize the GFP passenger protein. We also observed the endurance of the tag-fused proteins to heat treatment (see Supplemental Fig. 1 in supplementary material), suggesting the possibility of a simple purification protocol employing a heat treatment.

*Purification and characterization of tag-fused proteins*

To verify whether a large amount of tag protein can be obtained using a *T. th.* tag-mediated system, large-scale expression and purification were performed. Tth2- or Tth10-fused protein was used because these two tags could efficiently solubilize insoluble protein. After induction, the proteins were purified in two steps: using nickel–nitrilotriacetate (Ni–NTA) columns and through size exclusion (Fig. 5A). Despite the good expression, the Tth2–Vpr protein was harder to purify, probably owing to the residual insoluble properties derived from Vpr. Except for the Tth2–Vpr protein, at least 1 mg of pure protein was obtained from a 1-L culture. Meanwhile, because a high concentration of salt improved the solubility of tag-fused proteins, 0.5 M NaCl was added at all of the purification and analysis steps. CD spectra of purified proteins were measured. CD of the Tth2 protein showed the typical pattern of an α-helix-containing protein, which has negative maxima at 209 and 222 nm (Fig. 5B), consistent with the results of crystal structure of Tth2 protein (PDB ID: 1WF4). Other proteins fused with Tth2 proteins, such as Tth2–GFP, Tth2–Vpr, and Tth2–gp41-MSD, also

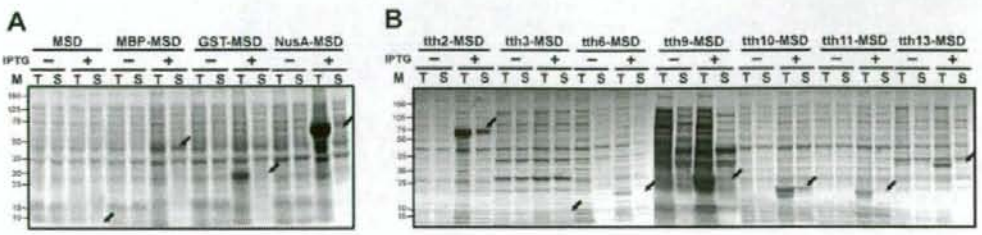


**Fig. 3.** Efficacy of tag protein for the expression of insoluble protein, gp41-MSD (MSD) from HIV-1. (A) Expression profiles of MSD alone and when fused with each of three conventional tags: MBP, GST, and NusA. (B) Expression profiles of tth-fused MSD. Each arrow indicates the position of the expected molecular weight of the fusion protein. Abbreviations are as defined in Fig. 2.

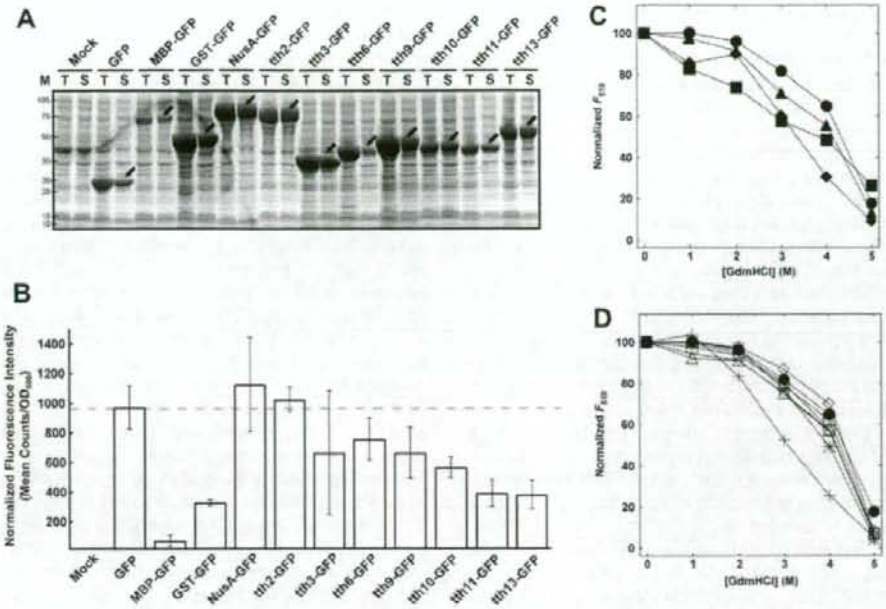


**Fig. 4.** Properties of tag-fused GFP. (A) Expression profile of tag-fused GFP. All cell extracts were prepared after 5 h exposure to 1 mM IPTG. Based on the calculated molecular weights, the positions of expected proteins are marked by arrows. Abbreviations are as defined in Fig. 2. (B) Fluorescence intensity of tag-fused GFP-expressing *E. coli* cells. The profiles of expression levels of GFP or tag-fused GFPs are the same as those in panel A. The measured mean fluorescence signal was normalized by dividing by the optical density of the culture at 600 nm. The standard deviations were calculated based on the results obtained in more than five independent experiments. (C,D) Residual intensity at 510 nm of proteins fused with conventional tags (C) or tth tags (D) and denatured by GdmHCl. Fluorescence intensities are expressed using nondenatured GFP as 100%. ●, tag-free GFP; ■, MBP-fused GFP; ▲, GST-fused GFP; ♦, NusA-fused GFP; ○, tth2-fused GFP; □, tth3-fused GFP; ◇, tth6-fused GFP; △, tth9-fused GFP; ▽, tth10-fused GFP; *, tth11-fused GFP; +, tth13-fused GFP.

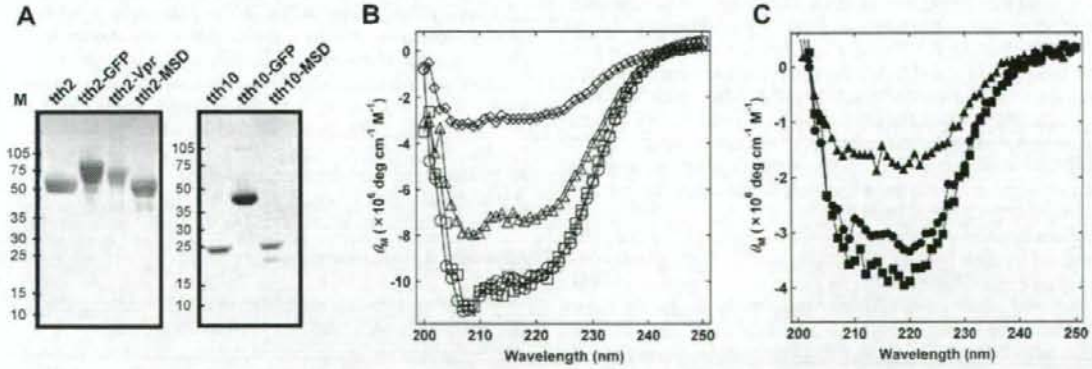


**Fig. 5.** Purification and secondary structure analyses of tag-fused proteins. (A) SDS–PAGE profile of purified proteins with MSD indicating gp41-MSD. (B) CD spectra of tth2-fused proteins. ○, tth2 alone; □, tth2-fused GFP; △, tth2-fused Vpr; ◇, tth2-fused MSD. (C) CD spectra of tth10-fused proteins. ●, tth10 alone; ■, tth10-fused GFP; ▲, tth10-fused MSD.

have similar negative maxima, suggesting that a considerable number of α-helical structures were present in the tag-fused proteins (Fig. 5B). The intensities of CD spectra for Tth2 and Tth2–GFP proteins were nearly identical, whereas those of Tth2–Vpr and Tth2–gp41-MSD proteins were lower. As for Tth10 and Tth10-fused proteins, the patterns of negative maxima were similar but the intensity of Tth10-fused gp41-MSD was reduced compared with that of Tth10 protein alone. Although it is difficult to explain the decrease in the intensities, the observed decreases may suggest that fusion-driven alterations to the proteins' structures occur.

## Discussion

In this study, we used the information on properties of the *T. th.* proteins accumulated during structural genomics studies to produce tag proteins that could facilitate the high production of target proteins. We applied two major criteria for the selection of the candidate tag proteins: high expression level and high solubility. The additional criterion, a high-resolution structure, was employed because this characteristic can facilitate phase determination during X-ray diffraction; the fused tag can be used as a template for molecular replacement. The 15 proteins that

met these criteria were diverse in their functions and structures (Table 1).

We examined the versatility of the selected tag proteins by fusing them to the highly insoluble adaptor protein Vpr. The candidate *T. th.* tag proteins showed themselves to be more effective when placed at the N terminus of Vpr (Fig. 2). The efficacies of the enhancements to protein expression proved to be nearly comparable to—or sometimes better than—those achieved with conventional tag proteins. Thus, the proteins derived from *T. th.* can be used as alternative tag proteins for efficient protein expression. Furthermore, we successfully identified one *T. th.* tag protein, Tth2, that could express Vpr in a soluble form. In addition to Tth2, the Tth10 protein could solubilize the extremely insoluble gp41-MSD (Figs. 2 and 3) more effectively than MBP, GST, or NusA.

When we tested Vpx as the fusion partner, the *T. th.* tag-fused proteins were expressed better than tag-free proteins, although the tagged proteins did not solubilize (data not shown). This apparent difference in solubility could arise from many factors other than the difference of the passenger proteins. One possible factor is the influence of the sequence that links the tag and the passenger protein. Indeed, we observed that some *T. th.* tags became insoluble when fused to a polyhistidine tag in our pET-47 vector (Fig. 2C). Others have observed similar effects of the linker sequence on expression and, possibly, solubility [12–14]. The linker sequence also plays an important role in the crystallization of a tag-fused protein [17]. Therefore, for successful analyses, it seems to be essential that both the fusion tag and linker sequence be carefully selected.

The high crystallization characteristics of *T. th.* proteins may confer additional advantage to this tag system. For this reason, we intended to retain the *T. th.* tag proteins after the purification not only to keep the proteins soluble but also to facilitate their crystallization. Therefore, we estimated the effects that the tag proteins had on the passenger proteins. Our analyses of tag-fused GFPs showed that 7 of the 15 candidate *T. th.* tags did not diminish either the function or the stability of GFP (Fig. 4). Even the considerable effect that the Tth2 protein had on the function of the passenger protein compared favorably with that produced with GST. In contrast, MBP had a considerable negative effect on the function of GFP; it also decreased the expression level of GFP itself. This effect has been reported previously [36]. Our results suggest that *T. th.* tags have similar or milder effects on the function of passenger proteins compared with the effects produced with the conventional tags MBP, GST, and NusA.

We focused mainly on the practical properties of *T. th.* proteins rather than on their biological functions when selecting our candidate tag proteins. Therefore, the two successful candidates identified for Vpr and gp41-MSD in this study have unrelated biochemical properties; Tth2 protein is the molecular chaperon GroEL, and Tth10 protein is the phosphotransferase adenylate kinase (Table 1). Each is known to undergo a conformational change on ligand binding [37–40], a characteristic suggesting that these proteins have flexible structures. In Fig. 5, the molar ellipticities of the fusion proteins, especially those fused with insoluble proteins, were not cumulative against the ellipticity of *T. th.* tag alone. The decrease in the intensities of the *T. th.* tag-fused insoluble proteins, such as Tth2–Vpr, Tth2–gp41-MSD, and Tth10–gp41-MSD, may reflect the structure alternation of the *T. th.* tag proteins for solubilization. There seems to be no severe structural alteration in the passenger protein; the fluorescent intensities of GFP and Tth2- or Tth10-fused GFP were nearly identical (Fig. 4).

In the case of Tth2 protein, the chaperon activity of GroEL may mediate the process of protein-folding and result in the efficient solubilization of the passenger protein [41]. Indeed, coexpression of GroEL/GroES for the production of target proteins in *E. coli* is widely used for the production of correctly folded proteins [42–46]. It has been reported, however, that GroEL from *T. th.* does not have chaperon activity alone [47]. If Tth2 protein acts as a molecular chaperon, endogenous GroES in *E. coli* may function in a coordinate manner during protein synthesis. At this point, we cannot explain the exact mechanism of Tth2-induced solubilization.

In this study, we have used the systematically accumulated data of the structural genomics project of *T. th.* to develop tag proteins useful for protein expression and solubilization. The properties used for the selection of candidate tags, such as high expression level and high solubility, are beneficial but do not necessarily guarantee that the protein will be a successful solubilizing partner. Although different proteins may need different fusion tags to achieve maximum efficacy of expression and solubility, it is noteworthy that the highly hydrophobic gp41-MSD could be solubilized with the use of *T. th.* tag. It is estimated that approximately 30% of all proteins are membrane proteins, and structural analysis of these proteins can be difficult because these proteins are often insoluble. The approach shown here may facilitate their structural analysis. Our preliminary trials of crystallization of *T. th.* tag-fused Vpr and gp41-MSD yielded small crystals. We are interested in determining whether the attached tag protein can facilitate phase determination during X-ray crystallographic analyses, as we have proposed. Moreover, investigation of this type must be useful because the greater the number of effective solubility-enhancing tags we can identify, the better are the chances of understanding the mechanism of solubility enhancement.

## Acknowledgments

This work was supported in part by the Program of Founding Research Centers for Emerging and Reemerging Infectious Diseases of the Ministry of Education, Culture, Sports, Science, and Technology (MEXT). We are grateful to the staff members of the Structural Biology Core Facility at the Institute of Biophysics, Chinese Academy of Sciences, for technical assistance. We thank Zhensheng Xie of Proteomic Platform at the Institute of Biophysics, Chinese Academy of Sciences, for identification of proteins with mass spectrometry. We thank Xinyu Wang for assistance with the Pistar instrument. We thank Kunito Yoshiike and Mark Bartlam for a critical reading of the manuscript. We also thank A. M. Menting, an editorial consultant, for preparation of the manuscript.

## Appendix A. Supplementary data

Supplementary data associated with this article can be found, in the online version, at doi:10.1016/j.ab.2008.10.050.

## References

[1] S.G. Dahl, I. Sylte, Molecular modeling of drug targets: The past, the present, and the future, Basic Clin. Pharmacol. Toxicol. 96 (2005) 151–155.
[2] K. Klumpp, T. Mirzadegan, Recent progress in the design of small molecule inhibitors of HIV RNase H, Curr. Pharm. Des. 12 (2006) 1909–1922.
[3] P. Beltrao, C. Kiel, L. Serrano, Structures in systems biology, Curr. Opin. Struct. Biol. 17 (2007) 378–384.
[4] M. Grabowski, A. Joachimiak, Z. Otwinowski, W. Minor, Structural genomics: keeping up with expanding knowledge of the protein universe, Curr. Opin. Struct. Biol. 17 (2007) 347–353.
[5] J. Weigelt, L.D. McBroom-Cerajewski, M. Schapira, Y. Zhao, C.H. Arrowmsmith, Structural genomics and drug discovery: all in the family, Curr. Opin. Chem. Biol. 12 (2008) 32–39.
[6] M.C. Smith, T.C. Furman, T.D. Ingolia, C. Pidgeon, Chelating peptide-immobilized metal ion affinity chromatography: a new concept in affinity chromatography for recombinant proteins, J. Biol. Chem. 263 (1988) 7211–7215.
[7] K. Terpe, Overview of tag protein fusions: from molecular and biochemical fundamentals to commercial systems, Appl. Microbiol. Biotechnol. 60 (2003) 523–533.

[8] D. Sachdev, J.M. Chirgwin, Fusions to maltose-binding protein: control of folding and solubility in protein purification, Methods Enzymol. 326 (2000) 312–321.
[9] D.B. Smith, Generating fusions to glutathione S-transferase for protein studies, Methods Enzymol. 326 (2000) 254–270.
[10] E.R. LaVallie, E.A. DiBlasio, S. Kovacic, K.L. Grant, P.F. Schendel, J.M. McCoy, A thioredoxin gene fusion expression system that circumvents inclusion body formation in the *E. coli* cytoplasm, Bio/Technology 11 (1993) 187–193.
[11] G.D. Davis, C. Elisee, D.M. Newham, R.G. Harrison, New fusion protein systems designed to give soluble expression in *Escherichia coli*, Biotechnol. Bioeng. 65 (1999) 382–388.
[12] R.B. Kapust, D.S. Waugh, *Escherichia coli* maltose-binding protein is uncommonly effective at promoting the solubility of polypeptides to which it is fused, Protein Sci. 8 (1999) 1668–1674.
[13] L. Niiranen, S. Espelid, C.R. Karlsen, M. Mustonen, S.M. Paulsen, P. Heikinheimo, N.P. Willassen, Comparative expression study to increase the solubility of cold adapted Vibrio proteins in *Escherichia coli*, Protein Expr. Purif. 52 (2007) 210–218.
[14] J.G. Marblestone, S.C. Edavettal, Y. Lim, P. Lim, X. Zuo, T.R. Butt, Comparison of SUMO fusion technology with traditional gene fusion systems: enhanced expression and solubility with SUMO, Protein Sci. 15 (2006) 182–189.
[15] S. Nallamsetty, D.S. Waugh, Solubility-enhancing protein MBP and NusA play a passive role in the folding of their fusion partners, Protein Expr. Purif. 45 (2006) 175–182.
[16] G.G. Privé, G.E. Verner, C. Weitzman, K.H. Zen, D. Eisenberg, H.R. Kaback, Fusion proteins as tools for crystallization: the lactose permease from *Escherichia coli*, Acta Crystallogr. D 50 (1994) 375–379.
[17] D.R. Smyth, M.K. Mrozkiewicz, W.J. Mcgrath, P. Listwan, B. Kobe, Crystal structures of fusion proteins with large-affinity tags, Protein Sci. 12 (2003) 1313–1322.
[18] J.P. Donahue, H. Patel, W.F. Anderson, J. Hawiger, Three-dimensional structure of the platelet integrin recognition segment of the fibrinogen gamma chain obtained by carrier protein-driven crystallization, Proc. Natl. Acad. Sci. USA 91 (1994) 12178–12182.
[19] B. Kobe, R.J. Center, B.E. Kemp, P. Poumbourios, Crystal structure of human T cell leukemia virus type 1 gp21 ectodomain crystallized as a maltose-binding protein chimera reveals structural evolution of retroviral transmembrane proteins, Proc. Natl. Acad. Sci. USA 96 (1999) 4319–4324.
[20] Y. Zhan, X. Song, G.W. Zhou, Structural analysis of regulatory protein domains using GST-fusion proteins, Gene 281 (2001) 1–9.
[21] E. Le Rouzic, N. Belaïdouni, E. Estrabaud, M. Morel, J.C. Rain, C. Transy, F. Margottin-Goguet, HIV-1 Vpr function is mediated by interaction with the damage specific DNA-binding protein DDB1, Cell Cycle 6 (2007) 182–188.
[22] B. Schrofelbauer, Y. Hakata, N.R. Landau, HIV-1 Vpr function is mediated by interaction with the damage specific DNA-binding protein DDB1, Proc. Natl. Acad. Sci. USA 104 (2007) 4130–4135.
[23] K. Hrecka, M. Gierszewska, S. Srivastava, L. Kozaczkiewicz, S.K. Swanson, L. Florensm, M.P. Washburn, J. Skowronski, Lentiviral Vpr usurps Cul4-DDB1[VprBP] E3 ubiquitin ligase to modulate cell cycle, Proc. Natl. Acad. Sci. USA 104 (2007) 11778–11783.
[24] X. Wen, K.M. Duus, T.D. Friedrich, C.M. de Noronha, The HIV-1 protein Vpr acts to promote G2 cell cycle arrest by engaging a DDB1 and Cullin4A-containing ubiquitin ligase complex using VprBP/DCAF1 as an adaptor, J. Biol. Chem. 282 (2007) 27046–27057.
[25] L. Tan, E. Ehrlich, X.F. Yu, DDB1 and Cul4A are required for human immunodeficiency virus type 1 Vpr-induced G2 arrest, J. Virol. 81 (2007) 10822–10830.
[26] E. Le Rouzic, S. Benichou, The Vpr protein from HIV-1: distinct roles along the viral life cycle, Retrovirology 2 (2005) 11.
[27] K. Miyauchi, J. Komano, Y. Yokomaku, W. Sugiura, N. Yamamoto, Z. Matsuda, Role of the specific amino acid sequence of the membrane-spanning domain of human immunodeficiency virus type 1 in membrane fusion, J. Virol. 79 (2005) 4720–4729.
[28] Structural–Biological Whole Cell Project. Available from: <http://www.thermus.org>.
[29] H. Iino, H. Naitow, Y. Nakamura, N. Nakagawa, Y. Agari, M. Kanagawa, A. Ebihara, A. Shikai, M. Sugahara, M. Miyano, N. Kamiya, S. Yokoyama, K. Hirotsu, S. Kuramitsu, Crystallization screening test for the Whole-Cell Project on *Thermus thermophilus* HB8, Acta Crystallogr. F 64 (2008) 487–491.
[30] T. Oshima, K. Imahori, Description of *Thermus thermophilus* (Yoshida and Oshima) comb. nov., a nonsporulating thermophilic bacterium from a Japanese thermal spa, Int. J. Syst. Bacteriol. 24 (1974) 102–112.
[31] S. Yokoyama, H. Hirota, T. Kigawa, T. Yabuki, M. Shirouzu, T. Terada, Y. Ito, Y. Matsuo, Y. Kuroda, Y. Nishimura, Y. Kyogoku, K. Miki, R. Masui, S. Kuramitsu, Structural genomics projects in Japan, Nat. Struct. Biol. 7 (2000) 943–945.
[32] RIKEN Bioresource Center DNA Bank, *Thermus thermophilus*. Available from: <http://www.brc.riken.jp/lab/dna/en/thermus_en.html>.
[33] S. Cabantous, T.C. Terwilliger, G.S. Waldo, Protein tagging and detection with engineered self-assembling fragments of green fluorescent protein, Nat. Biotechnol. 23 (2005) 102–107.
[34] P. Henklein, K. Bruns, M.P. Sherman, U. Tessmer, K. Licha, J. Kopp, C.M. de Noronha, W.C. Greene, V. Wray, U. Schubert, Functional and structural characterization of synthetic HIV-1 Vpr that transduces cells, localizes to the nucleus, and induces G2 cell cycle arrest, J. Biol. Chem. 275 (2000) 32016–32026.
[35] L. Slabinski, L. Jaroszewski, A.P. Rodrigues, L. Rychlewski, I.A. Wilson, S.A. Lesley, A. Godzik, The challenge of protein structure determination lessons from structural genomics, Protein Sci. 16 (2007) 247–282.
[36] A.H. Podmore, P.E. Reynolds, Purification and characterization of VanXYC, a D,D-dipeptidase/D,D-carboxypeptidase in vancomycin-resistant *Enterococcus gallinarum* BM4174, Eur. J. Biochem. 269 (2002) 2740–2746.
[37] M. Taniguchi, T. Yoshimi, K. Hongo, T. Mizobata, Y. Kawata, Stopped-flow fluorescence analysis of the conformational changes in the GroEL apical domain: relationships between movements in the apical domain and the quaternary structure of GroEL, J. Biol. Chem. 279 (2004) 16368–16376.
[38] M. Yokokawa, C. Wada, T. Ando, N. Sakai, A. Yagi, S.H. Yoshimura, K. Takeyasu, Fast-scanning atomic force microscopy reveals the ATP/ADP-dependent conformational changes of GroEL, EMBO J. 25 (2006) 4567–4576.
[39] K. Arora, C.L. Brooks III, Large-scale allosteric conformational transitions of adenylate kinase appear to involve a population-shift mechanism, Proc. Natl. Acad. Sci. USA 104 (2007) 18496–18501.
[40] P.C. Whitford, S. Gosavi, J.N. Onuchic, Conformational transitions in adenylate kinase: allosteric communication reduces misligation, J. Biol. Chem. 283 (2008) 2042–2048.
[41] A.L. Horwich, G.W. Farr, W.A. Fenton, GroEL–GroES-mediated protein folding, Chem. Rev. 106 (2006) 1917–1930.
[42] P. Goloubinoff, A.A. Gatenby, G.H. Lorimer, GroE heat-shock proteins promote assembly of foreign prokaryotic ribulose bisphosphate carboxylase oligomers in *Escherichia coli*, Nature 337 (1989) 44–47.
[43] S.C. Lee, P.O. Olins, Effect of overproduction of heat shock chaperones GroESL and DnaK on human procollagenase production in *Escherichia coli*, J. Biol. Chem. 267 (1992) 2849–2852.
[44] P. Caspers, M. Stieger, P. Burn, Overproduction of bacterial chaperones improves the solubility of recombinant protein tyrosine kinases in *Escherichia coli*, Cell. Mol. Biol. 40 (1994) 635–644.
[45] K.E. Amrein, B. Takacs, M. Stieger, J. Molnos, N.A. Flint, P. Burn, Purification and characterization of recombinant human p50csk protein–tyrosine kinase from an *Escherichia coli* expression system overproducing the bacterial chaperones GroES and GroEL, Proc. Natl. Acad. Sci. USA 92 (1995) 1048–1052.
[46] K. Nishihara, M. Kanemori, H. Yanagi, T. Yura, Overexpression of trigger factor prevents aggregation of recombinant proteins in *Escherichia coli*, Appl. Environ. Microbiol. 66 (2000) 884–889.
[47] K. Amada, M. Yohda, M. Odaka, I. Endo, N. Ishii, H. Taguchi, M. Yoshida, Molecular cloning, expression, and characterization of chaperonin-60 and chaperonin-10 from a thermophilic bacterium, *Thermus thermophilus* HB8, J. Biochem. 118 (1995) 347–354.

Available online at www.sciencedirect.com
ScienceDirect
VIROLOGY
Virology 373 (2008) 447–456
www.elsevier.com/locate/yviro

# Comparison of anti-viral activity of rhesus monkey and cynomolgus monkey TRIM5αs against human immunodeficiency virus type 2 infection

Ken Kono, Haihan Song, Yasuhiro Shingai, Tatsuo Shioda, Emi E. Nakayama *

*Department of Viral Infections, Research Institute for Microbial Diseases, Osaka University, 3-1, Yamada-oka, Suita-shi, Osaka 565-0871, Japan*

Received 9 November 2007; returned to author for revision 28 November 2007; accepted 17 December 2007
Available online 21 February 2008

**Abstract**

Human immunodeficiency virus type 2 (HIV-2) strains vary widely in their ability to grow in Old World monkey (OWM) cells. We previously evaluated several HIV-2 isolates for their sensitivity to cynomolgus monkey (CM) TRIM5α, an anti-HIV factor in OWM cells, and found that viruses carrying proline at the 120th position of the capsid protein were sensitive to CM TRIM5α, whereas those with either alanine or glutamine were resistant. In the study presented here, we tested these HIV-2 isolates for their sensitivity to rhesus monkey (Rh) TRIM5α and found that both CM TRIM5α-sensitive and -resistant viruses were restricted by Rh TRIM5α. The variable region 1 of the SPRY domain of Rh TRIM5α appeared to be the determinant of this difference. Furthermore, a mutagenesis study showed that three amino acid residues TFP at the 339th to 341st positions of Rh TRIM5α are important for restricting HIV-2 strains resistant to CM TRIM5α.


*Keywords:* TRIM5α; Human immunodeficiency virus; Rhesus monkey; Cynomolgus monkey

## Introduction

Human immunodeficiency virus type 1 (HIV-1) has a very narrow host range limited to humans and chimpanzees. Experiments have demonstrated that HIV-1 does not infect Old World monkeys (OWM) such as rhesus and cynomolgus monkeys. Recently, the screening of a rhesus monkey cDNA library identified tripartite motif 5α (TRIM5α) as a factor that confers resistance to HIV-1 infection (Stremlau et al., 2004). Rhesus and cynomolgus monkey TRIM5α restricts HIV-1 infection (Stremlau et al., 2004; Yap et al., 2004; Nakayama et al., 2005), whereas human TRIM5α restricts N-tropic murine leukemia virus (N-MLV) infection (Hatziioannou et al., 2004; Keckesova et al., 2004; Perron et al., 2004). African green monkey (AGM) TRIM5α restricts simian immunodeficiency virus isolated from a macaque monkey (SIVmac), human immunodeficiency virus type 2 (HIV-2), and equine infectious anemia virus in addition to HIV-1 infection (Hatziioannou et al., 2004; Keckesova et al., 2004; Nakayama et al., 2005). TRIM5α shares with other splicing variants a common amino-terminal TRIM motif, comprising RING, B-box and coiled-coil domains, and encodes a unique SPRY (B30.2) domain (Reymond et al., 2001). Several recombinant studies of human and rhesus monkey TRIM5α have shown that the determinant of the species specificity lies in the SPRY domain of TRIM5α (Perez-Caballero et al., 2005; Sawyer et al., 2005; Stremlau et al., 2005; Yap et al., 2005). We also previously demonstrated that 17-amino-acid residues and adjacent AGM-specific 20-amino-acid duplication in the SPRY domain determined species-specific restriction of SIVmac (Nakayama et al., 2005). It is known that the RING and B-box domains are required for restriction and that the coiled-coil domain is required for multimerization (Stremlau et al., 2004; Berthoux et al., 2005; Perez-Caballero et al., 2005; Nakayama et al., 2006). TRIM5α is thought to bind HIV capsid and promote its rapid, premature disassembly in ubiquitin dependent

* Corresponding author. Fax: +81 6 6879 8347.
*E-mail address:* emien@biken.osaka-u.ac.jp (E.E. Nakayama).

0042-6822/$ - see front matter © 2007 Elsevier Inc. All rights reserved.
doi:10.1016/j.virol.2007.12.022

and independent manners (Stremlau et al., 2006; Diaz-Griffero et al., 2006; Wu et al., 2006; Anderson et al., 2006). This means that the viral RNA and proteins are exposed to cellular proteins and degraded before nuclear transportation.

HIV-2 has a genome extremely similar to that of SIVmac (Hahn et al., 2000). In contrast with the many reports concerning HIV-1 and SIVmac, there have been only a few on susceptibility of HIV-2 to TRIM5α from various species (Nakayama et al., 2005; Ylinen et al., 2005). We previously evaluated eight HIV-2 isolates for their sensitivity to cynomolgus monkey TRIM5α and found that viruses carrying proline at the 119th or 120th position of the capsid protein (CA) were sensitive to cynomolgus monkey TRIM5α, whereas those with either alanine or glutamine were resistant (Song et al., 2007). In the study presented here, we tested these HIV-2 isolates for their sensitivity to another OWM rhesus monkey TRIM5α and found that both cynomolgus monkey TRIM5α-sensitive and -resistant viruses were restricted by rhesus monkey TRIM5α. We were able to show that three amino acid residues TFP at the 339th to 341st positions of rhesus monkey TRIM5α are important for restriction activity against HIV-2 strains.

## Results

### *Rhesus monkey TRIM5 inhibits both cynomolgus monkey TRIM5 -sensitive and -resistant HIV-2 viruses*

We previously reported that HIV-2 isolates carrying proline at the 120th position of CA were sensitive to cynomolgus monkey TRIM5α, whereas those with either alanine or glutamine were resistant. Both cynomolgus and rhesus monkey TRIM5αs are known to restrict HIV-1 but not SIVmac. Predicted amino acid sequences of cynomolgus and rhesus monkey TRIM5α are shown in Fig. 1. Rhesus and cynomolgus monkey TRIM5α share 96.8% of amino acid residues. To test these HIV-2 isolates for their sensitivity to rhesus monkey TRIM5α, we constructed a recombinant Sendai virus (SeV) expressing rhesus monkey TRIM5α fused with the HA tag in the C-terminal. Western blot analysis using an antibody against HA-tag showed that rhesus monkey TRIM5α was expressed at similar levels to those of cynomolgus monkey TRIM5α in recombinant SeV infected human T-cell line MT4 cells (data not shown). Fluorescent microscopic observation confirmed that these TRIM5αs were detected in all the cells infected with recombinant SeVs (data not

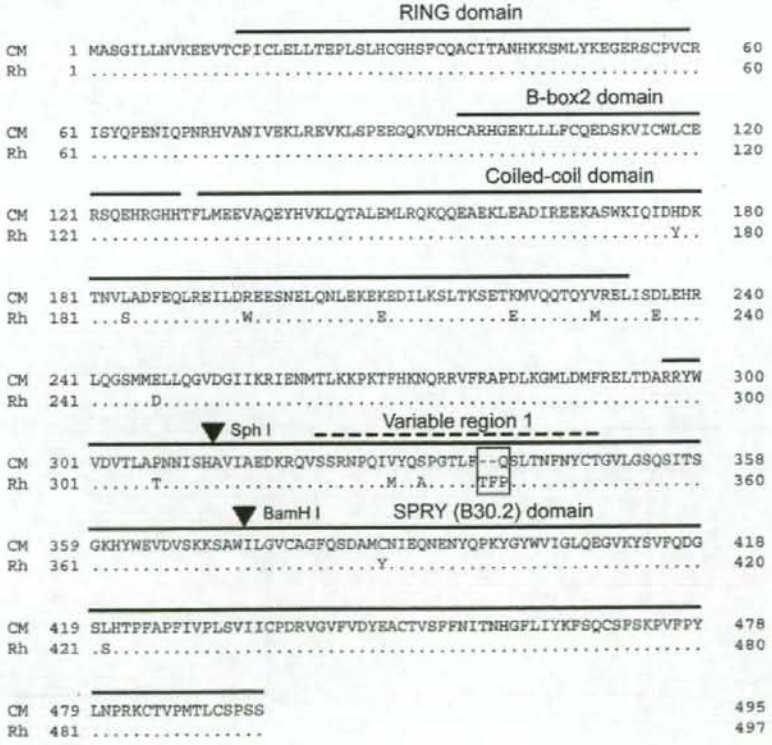


Fig. 1. Alignments of amino acid sequences of cynomolgus monkey (CM) and rhesus monkey (Rh) TRIM5αs. The RING, B-box2, coiled-coil and SPRY (B30.2) domains are indicated by labeled bars over the sequence. Variable region 1 is indicated by a broken bar over the sequence. Dots denote the amino acid residues identical to the one of cynomolgus monkey TRIM5α and dashes a lack of the amino acid residue that is present in rhesus monkey TRIM5α. The box marks amino acid residues that are important for rhesus monkey TRIM5α restriction activity against HIV-2 strains (see Results).

shown). We used SeV expressing cynomolgus monkey TRIM5α lacking the SPRY domain, CM SPRY( ) TRIM5α, as a negative control. MT4 cells infected with recombinant SeV expressing rhesus monkey TRIM5α, cynomolgus monkey TRIM5α, or CM SPRY( ) TRIM5α were then superinfected with an X4-tropic HIV-1 strain NL43, SIVmac239, HIV-2 strain GH123, or GH123/Q which is a mutant HIV-2 carrying glutamine (Q) at the 120th position of CA. In agreement with the results of previous studies, rhesus and cynomolgus monkey TRIM5α could restrict HIV-1 NL43, but failed to restrict SIVmac239 (Fig. 2, upper panels). HIV-2 GH123, cynomolgus monkey TRIM5α-sensitive strain, was restricted by both rhesus and cynomolgus monkey TRIM5αs (Fig. 2, lower left panel), which is also consistent with the findings of previous studies (Song et al., 2007). Despite a high degree of sequence similarity between rhesus and cynomolgus monkey TRIM5αs, rhesus monkey TRIM5α could inhibit replication of HIV-2 GH123/Q, the strain resistant to cynomolgus monkey TRIM5α (Fig. 2, lower right panel).

*Variable region 1 (V1) of SPRY (B30.2) domain of rhesus monkey TRIM5 is a determinant for restriction of HIV-2 GH123/Q infection*

It is known that the variable region 1 (V1) (Song et al., 2005a,b) of the rhesus monkey TRIM5α SPRY domain is the major determinant of anti-HIV-1 potency (Perez-Caballero et al., 2005; Sawyer et al., 2005; Stremlau et al., 2005; Yap et al., 2005). To determine the precise region of TRIM5α responsible for the anti HIV-2 GH123/Q activity of rhesus monkey TRIM5α, we constructed a recombinant SeV expressing chimeric TRIM5αs between rhesus and cynomolgus monkey TRIM5α by using *Sph*I and *Bam*HI restriction enzyme digestion (Fig. 3A). The central fragment comes from *Sph*I and *Bam*HI digestion contains the V1 of SPRY domain (Fig. 1).

As expected, all forms of chimeric TRIM5α inhibited HIV-1 NL43 and HIV-2 GH123 replication, although the extent of inhibition of HIV-2 GH123 varied among chimeric TRIM5αs (Fig. 3B, left and center panel). On the other hand, 212, 112, and 211 chimeric TRIM5α restricted HIV-2 GH123/Q infection, whereas 121, 221, and 122 chimeric TRIM5α did not (Fig. 3B, right panel), although the expression levels of the latter 1 day after SeV infection were not lower than those of parental and other chimeric TRIM5αs (Fig. 3C). Furthermore, these chimeric TRIM5α expression levels at day 6 after SeV infection were almost equivalent to those at day 1 after SeV infection (data not shown). These results confirmed that stability and kinetics of expression were similar among these chimeric TRIM5αs. Since 212,112, and 211 chimeric TRIM5α possess the rhesus monkey TRIM5α V1, those results indicated that the rhesus monkey TRIM5α V1 is a determinant of anti HIV-2 GH123/Q activity. It is noteworthy that cynomolgus monkey TRIM5α-sensitive HIV-2 GH123 grew to slightly higher titers in the cells

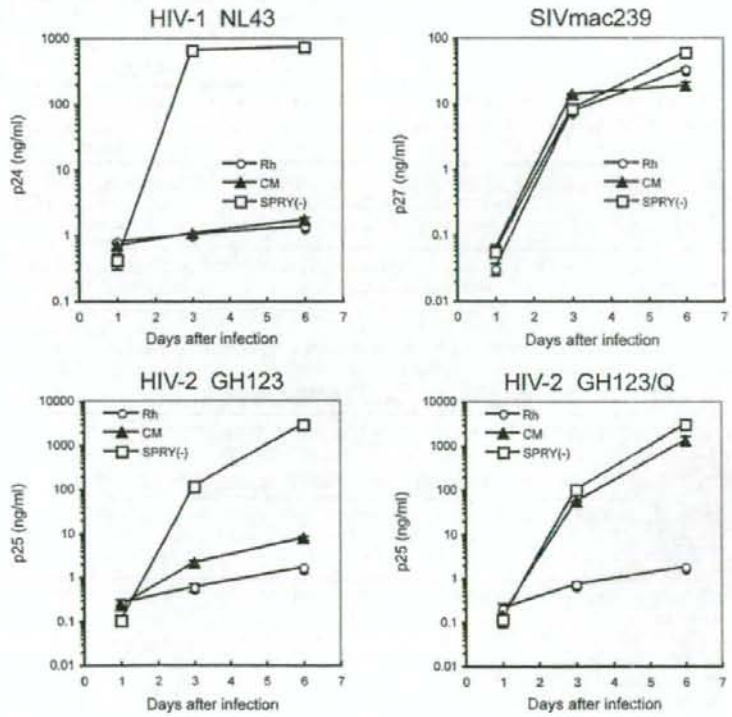


Fig. 2. MT4 cells infected with recombinant SeV expressing rhesus monkey (Rh; ), cynomolgus monkey (CM; ), or CM SPRY( )( ) TRIM5α were inoculated with HIV-1 NL43, SIVmac239, HIV-2 GH123, or HIV-2 GH123/Q. Culture supernatants were respectively assayed for levels of p24, p27, or p25. HIV-2 GH123/Q is a mutant virus carrying glutamine (Q) at the 120th position of HIV-1 GH123 capsid. CM SPRY( ) TRIM5α served as negative control.

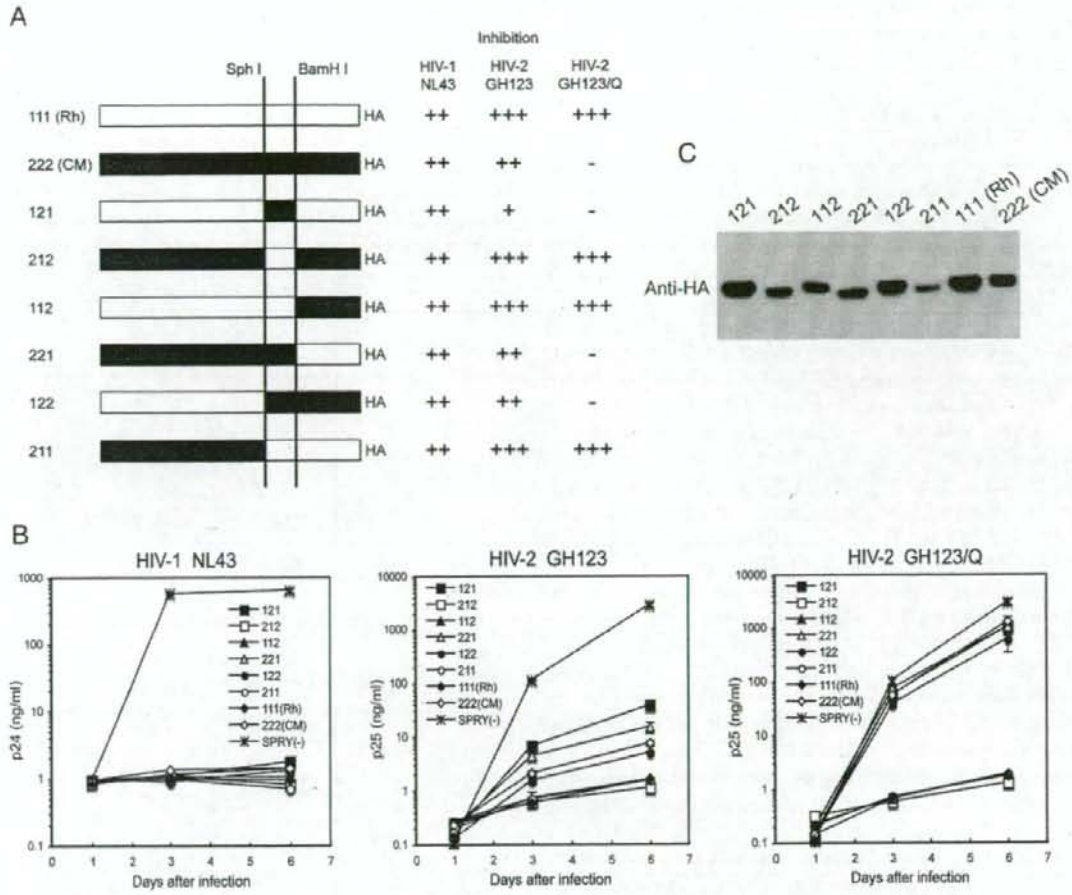


Fig. 3. (A) Schematic representation of chimeric TRIM5αs and summary of the results. White and black bars denote rhesus monkey (Rh) and cynomolgus monkey (CM) sequences, respectively. +++, ++, +, and denote more than 1000-fold, 100- to 1000-fold, 8- to 100-fold, and less than 8-fold suppression of virus growth, respectively, compared with the negative control on day 6. (B) MT4 cells were infected with recombinant SeV expressing 121 ( ), 212 ( ), 112 ( ), 221 ( ), 122 ( ), 211 ( ), 111 (Rh) ( ), 222 (CM) ( ), or CM SPRY( ) (*) TRIM5α. Nine hours after infection, cells were inoculated with HIV-1 NL43, HIV-2 GH123, or HIV-2 GH123/Q viruses. Culture supernatants were respectively assayed for levels of p24 or p25. (C) Twenty-four hours after SeV infection, TRIM5α proteins in lysates of MT4 cells infected with recombinant SeV expressing 121, 212, 112, 221, 122, 211, 111 (Rh), or 222 (CM) TRIM5α were visualized by Western blotting with an antibody against HA-tag.

expressing chimeric 121 or 221 TRIM5α than in those expressing parental cynomolgus monkey or 122 chimeric TRIM5α (Fig. 3B, center panel). These results indicate that the extent of inhibition of HIV-2 GH123 by chimeric 121 and 221 TRIM5αs is slightly less than that by parental cynomolgus monkey and 122 chimeric TRIM5α. It has been reported that all three variable regions (V1–V3) could contribute to the anti-viral activity of TRIM5α (Ohkura et al., 2006). It is possible that the combination of the cynomolgus monkey TRIM5α V1 and the rhesus monkey TRIM5α C-terminal portion of the SPRY domain slightly impairs the anti-HIV-2 function of TRIM5α.

*V1 of SPRY domain of rhesus monkey TRIM5 is a determinant for broader and more potent anti-HIV-2 activity*

To examine the restriction activities of rhesus monkey TRIM5α against other HIV-2 strains, we tested HIV-2 UC2, HIV-2 UC12, and HIV-2 UC14 for their growth potential in human T-cell line Hut78 infected with SeV expressing 121, 212, 111 (rhesus monkey; Rh), 222 (cynomolgus monkey; CM), or SPRY( ) TRIM5α. As shown in Fig. 4, rhesus monkey TRIM5α and cynomolgus monkey chimeric TRIM5α containing the V1 of rhesus monkey TRIM5α (212) completely restricted HIV-2 UC2 and HIV-2 UC14, whereas cynomolgus monkey TRIM5α and rhesus monkey chimeric TRIM5α containing the V1 of cynomolgus monkey TRIM5α (121) failed to do so. Rhesus monkey TRIM5α and 212 chimeric TRIM5α also completely restricted HIV-2 UC12, while cynomolgus monkey TRIM5α did so partially, which is consistent with our previous findings (Song et al., 2007). 121 chimeric TRIM5α showed very weak restriction activity on replication of HIV-2 UC12. Putting these findings together leads us to conclude that the V1 is a determinant for broader and more potent anti-HIV-2 activity of rhesus monkey TRIM5α.

*Amino acid residues TFP at the 339th to 341st positions of rhesus monkey TRIM5 are important for inhibiting HIV-2 GH123/Q replication*

As shown in Fig. 1, the V1 of the SPRY domain of rhesus monkey TRIM5α contains two amino acid residues TF that are not present in cynomolgus monkey TRIM5α. To examine whether these two additional amino acid residues are responsible for the broad anti-HIV-2 activity of rhesus monkey TRIM5α, we constructed a recombinant SeV expressing rhesus monkey TRIM5α lacking these two amino acid residues (Rh deltaTF TRIM5α). We also constructed a SeV expressing mutant rhesus monkey TRIM5α in which amino acid residues TFP at the 339th to 341st positions were replaced with a single amino acid Q found in cynomolgus monkey TRIM5α (Rh TFP-Q TRIM5α) (Fig. 5A). Expression levels of mutant TRIM5αs in MT4 cells infected with these SeVs were comparable to those of parental TRIM5αs (Fig. 5B).

As shown in Fig. 5C, both of the mutant rhesus monkey TRIM5αs restricted HIV-1 infection. In the case of HIV-2, Rh deltaTF TRIM5α inhibited both HIV-2 GH123 and HIV-2 GH123/Q replications, although anti-HIV-2 activity was slightly weaker than that of parental rhesus monkey TRIM5α. On the other hand, Rh TFP-Q TRIM5α lost its inhibitory activity against HIV-2 GH123/Q, while it could suppress replication of HIV-2 GH123 to the same extent as it was suppressed by 121 chimeric TRIM5α. Conversely, cynomolgus monkey TRIM5α possessing TFP instead of Q at the 339th position (CM Q-TFP TRIM5α) completely restricted HIV-2 GH123/Q replication (Fig. 5D). These results indicated that these three amino acids are important for restricting HIV-2 GH123/Q by rhesus monkey TRIM5α.

*Baboon TRIM5 V1 confers anti-viral activity against HIV-2 GH123/Q to cynomolgus monkey TRIM5 , whereas sooty mangabey and pig-tailed monkey TRIM5 V1 fail to do so*

HIV-2 is thought to originate from the simian immunodeficiency virus of sooty mangabeys (Hahn et al., 2000). Several HIV-2 isolates could grow in baboon and pig-tailed monkey, and some of them were reported to cause an AIDS-like disease in these animals (Barnett et al., 1994; Locher et al., 1998; Locher et al., 2001; McClure et al., 2000). To assess anti-HIV-2 activity of these OWMs TRIM5αs, we constructed a recombinant SeV expressing cynomolgus monkey chimeric TRIM5α containing the V1 of baboon (2B2), sooty mangabey (2S2), or pig-tailed monkey (2P2) TRIM5α (Fig. 6A). Expression levels of these chimeric TRIM5αs in MT4 cells infected with the SeVs were comparable to those of parental cynomolgus monkey TRIM5α (Fig. 6C). The amino acid sequences of the V1 of baboon, sooty mangabey, and pig-tailed monkey TRIM5α are shown in Fig. 6B. Baboon and sooty mangabey TRIM5α show the SFP sequence at the 339th to 341st positions, whereas pig-tailed monkey TRIM5α has a single Q as cynomolgus monkey TRIM5α. As shown in Fig. 6D, all the chimeric TRIM5αs containing the V1 of baboon, sooty mangabey, and pig-tailed monkey TRIM5α restricted HIV-1 infection. These results are consistent with those of previous studies (Kaiser et al., 2007; Newman et al., 2006; Ohkura et al., 2006). In the case of HIV-2, there were wide variations in anti-HIV-2 activity by the chimeric TRIM5αs. Chimeric TRIM5α containing baboon V1 inhibited both HIV-2 GH123 and HIV-2 GH123/Q replications, while chimeric TRIM5α containing sooty mangabey V1 partially inhibited HIV-2 GH123 and only slightly inhibited HIV-2 GH123/Q replication. Finally, chimeric TRIM5α containing pig-tailed monkey V1 only slightly inhibited both HIV-2 GH123 and HIV-2 GH123/Q replication. This shows that there is a lack of correlation between the effects of various TRIM5αs on HIV-2

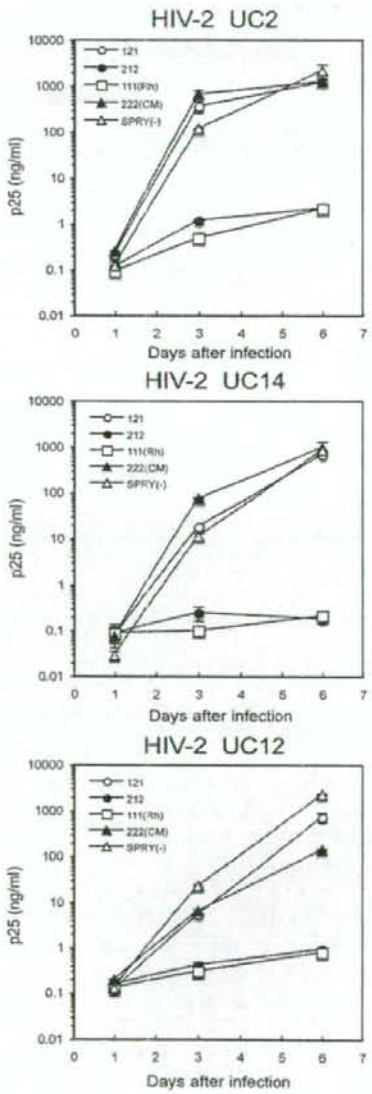


Fig. 4. Hut78 cells infected with recombinant SeV expressing 121 ( ), 212 ( ), 111 (Rh) ( ), 222 (CM) ( ) or CM SPRY( ) ( ) TRIM5α. Cells were super-infected with HIV-2 isolates, UC2, UC14, or UC12. Culture supernatants were assayed for levels of p25.

A

| | Amino acid sequence | Inhibition HIV-1 NL43 | HIV-2 GH123 | HIV-2 GH123/Q |
|---|---|---|---|---|
| Rh | QIMTQAPGTLPTFPSLN | ++ | +++ | +++ |
| CM | ..V..S.....--Q... | ++ | ++ | - |
| Rh deltaTF | ..........--.... | ++ | ++ | ++ |
| Rh TFP-Q | ..........--Q... | ++ | ++ | - |
| CM Q-TFP | ..V..S.......... | ++ | +++ | +++ |

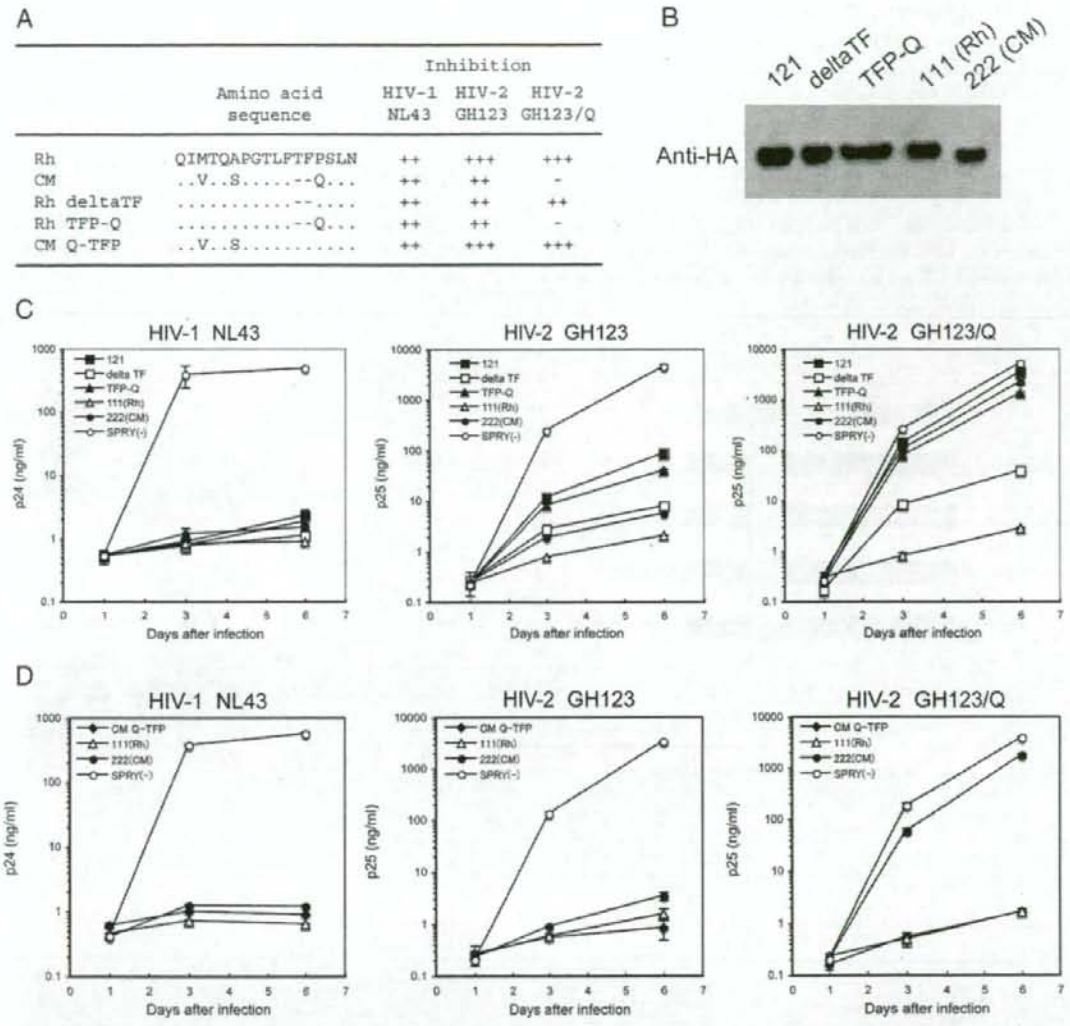


Fig. 5. (A) Mutant Rh deltaTF TRIM5α was generated by deleting 339th-TF-340th and mutant Rh TFP-Q TRIM5α was generated by replacing 339th-TFP-341st with Q by site-directed mutagenesis. Dots denote amino acid identity, dashes a lack of the amino acids residue present only in rhesus monkey (Rh) TRIM5α, and +++, ++, +, and – more than 1000-fold, 100- to 1000-fold, 8- to 100-fold, and less than 8-fold suppression of virus growth, respectively, compared with the negative control on day 6. (B) Twenty-four hours after SeV infection, TRIM5α proteins in lysates of MT4 cells infected with recombinant SeV expressing 121, Rh delta TF, Rh TFP-Q, 111 (Rh), or 222 (CM) TRIM5α were visualized by Western blotting with an antibody against HA-tag. (C) MT4 cells were infected with recombinant SeV expressing 121 ( ), Rh delta TF ( ), Rh TFP-Q ( ), 111 (Rh) ( ), 222 (CM) ( ), or CM SPRY( ) ( ) TRIM5α. Nine hours after infection, cells were inoculated with HIV-1 NL43, HIV-2 GH123, or HIV-2 GH123/Q viruses. Culture supernatants were respectively assayed for levels of p24 or p25. (D) MT4 cells were infected with recombinant SeV expressing CM Q-TFP ( ), 111 (Rh) ( ), 222 (CM) ( ), or CM SPRY( ) ( ) TRIM5α. Nine hours after infection, cells were inoculated with HIV-1 NL43, HIV-2 GH123, or HIV-2 GH123/Q viruses. Culture supernatants were respectively assayed for levels of p24 or p25.

and their reported ability to grow in these primate peripheral blood mononuclear cells.

## Discussion

In the study presented here, we found that rhesus monkey TRIM5α showed anti-HIV-2 activity broader and more potent than that of cynomolgus monkey. We were also able to show that three amino acid residues TFP at the 339th to 341st positions in the V1 were important for the broad HIV-2 restriction activity of rhesus monkey TRIM5α. Previous studies have shown that the V1 of TRIM5α determines species-specific restriction of HIV-1 and SIVmac (Perez-Caballero et al., 2005; Sawyer et al., 2005; Stremlau et al., 2005; Yap et al., 2005; Nakayama et al., 2005). Ours is the first study to demonstrate that the V1 of TRIM5α also determines anti-HIV-2 potency. Since MT4 and Hut78 cells express endogenous human TRIM5α, it is possible that endogenous human TRIM5α interfere with exogenous TRIM5α. However, the expression level of SeV-derived TRIM5α is more than 100 times higher than that of endogenous TRIM5α (data

not shown), and the effect of endogenous TRIM5α is therefore considered to be negligible.

A previous study using a human and rhesus monkey chimeric TRIM5α revealed that a single amino acid substitution from R to P at the 332nd position of human TRIM5α (corresponding to the 334th position in rhesus monkey TRIM5α) confers strong anti-HIV-1 activity to human TRIM5α (Stremlau et al., 2005; Yap et al., 2005). We found that rhesus monkey TRIM5α and chimeric TRIM5α containing baboon V1 strongly restricted HIV-2 GH123/Q, while chimeric TRIM5α containing sooty mangabey V1 did so only slightly, although baboon and sooty mangabey TRIM5α share the SFP motif at the 339th to 341st positions. Rhesus monkey and baboon TRIM5α possess P, whereas human and sooty mangabey TRIM5α possess R at the 334th position. On the other hand, cynomolgus monkey TRIM5α strongly restricted HIV-2 GH123, while chimeric TRIM5α containing pig-tailed monkey V1 did so only slightly. Cynomolgus monkey TRIM5α possesses P, whereas pig-tailed monkey TRIM5α possesses Q at the 334th position. These results indicate the P residue at the 334th position of primate TRIM5α also plays a critical role in the restriction of HIV-2.

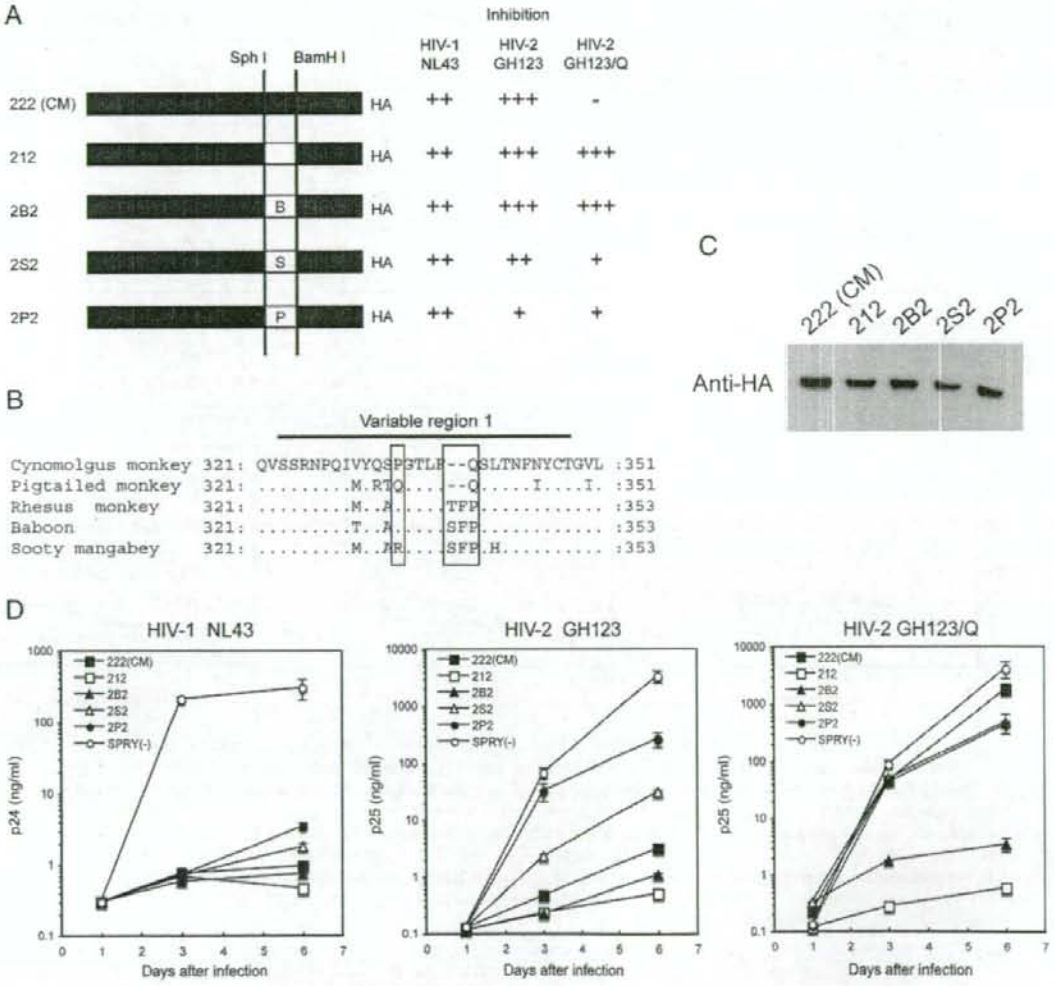


Fig. 6. (A) Schematic representation of chimeric TRIM5α and summary of the results. White and black bars denote rhesus monkey and cynomolgus monkey (CM) sequences, respectively. B, S, and P denote sequence from baboon, sooty mangabey, and pig-tailed monkey, respectively, and +++, ++, +, and - more than 1000-fold, 100- to 1000-fold, 8- to 100-fold, and less than 8-fold suppression of virus growth, respectively, compared with the negative control on day 6. (B) Alignment of amino acid sequences of the V1 and franking region within the SPRY domain of cynomolgus monkey, pigtailed monkey, rhesus monkey, baboon, and sooty mangabey TRIM5αs. V1 is indicated by a bar over the sequence. The first box indicates the amino acid residues that were referred to as site 332 in the human TRIM5α. The second box indicates amino acid residues that are important for restricting HIV-2 strains which are resistant to cynomolgus monkey TRIM5α. (C) Twenty-four hours after SeV infection, TRIM5α proteins in lysates of MT4 cells infected with recombinant SeV expressing 222 (CM), 212, 2B2, 2S2, or 2P2 TRIM5α were visualized by Western blotting with an antibody against HA-tag. (D) MT4 cells were infected with recombinant SeV expressing 222 (CM) ( ), 212 ( ), 2B2 ( ), 2S2 ( ), 2P2 ( ), or CM SPRY( ) ( ) TRIM5α. Nine hours after infection, cells were inoculated with HIV-1 NL43, HIV-2 GH123, or HIV-2 GH123/Q, viruses. Culture supernatants were respectively assayed for levels of p24 or p25.

HIV-2 is thought to have originated from the SIV from sooty mangabey (SIVsmm) (Hahn et al., 2000). Our results showed that HIV-2 GH123 replication was partially inhibited by chimeric TRIM5α containing sooty mangabey V1, while HIV-2 GH123/Q grew strongly in the presence of the chimeric TRIM5α. This result is consistent with the fact that all SIVsmm sequences in the Los Alamos database possess Q or A at the 119th or 120th position of CA (Song et al., 2007). On the other hand, chimeric TRIM5α containing sooty mangabey V1 has a strong anti-HIV-1 activity, even though it has R at the 334th position as in human TRIM5α. Sooty mangabey TRIM5α, on the other hand, possesses the SFP motif at the 339th to 341st positions. Yap et al. (2005) showed that human TRIM5α carrying the rhesus monkey sequence LFTFPSLT which included the TFP motif instead of the human sequence RYQTFV at the 335th to 340th positions could restrict HIV-1. These results thus indicate that the TFP or SFP motif at the 339th to 341st positions can confer anti-HIV-1 activity as well as the P residue at the 334th position.

In the case of pig-tailed monkey, which could develop an AIDS-like disease by HIV-2 (McClure et al., 2000), anti-HIV-2 activity of chimeric TRIM5α containing pig-tailed monkey V1 was very weak. Furthermore, after we completed this study, it was reported that pig-tailed monkeys lack expression of TRIM5α. Instead, pig-tailed monkeys express TRIM5θ and TRIM5η, novel TRIM5 isoforms lacking anti-HIV-1 activity (Brennan et al., 2007). These findings are probably account for the fact that pig-tailed monkey can be used as an AIDS model.

Previous studies showed that rhesus monkey as well as baboon can be infected with HIV-2 (Dormant et al., 1989; Franchini et al., 1989; Nicol et al., 1989; Franchini et al., 1990; Castro et al., 1991), while the latter can also develop an AIDS-like disease as a result of HIV-2 infection (Barnett et al., 1994; Locher et al., 1998; Locher et al., 2001). In our study, however, rhesus monkey TRIM5α and chimeric TRIM5α containing baboon V1 could strongly inhibit HIV-2 replication. The reason why HIV-2 can replicate in rhesus monkey and baboon, even though the TRIM5α of these monkey species possesses strong anti-HIV-2 activity, is unclear at present. The presence of TRIM5α mRNA in cells of rhesus monkey and baboon cells has been confirmed (Stremlau et al., 2004; Kaiser et al., 2007). It is also known that TRIM5α exhibits a high degree of sequence variation even within species. In rhesus monkey, there is a 339th-TFP-341st to Q polymorphism which diminishes the anti HIV-2 GH123/Q activity of rhesus monkey TRIM5α (Newman et al., 2006) (Fig. 5). It is thus possible that rhesus monkey carrying this polymorphism in the TRIM5α gene could be infected with HIV-2 and that a number of baboons have similar polymorphisms. It would be interesting to investigate the effect of genetic polymorphisms in baboon TRIM5α on its restriction activity against HIV-2.

## Materials and methods

### *Cloning and expression of TRIM5*

Rhesus monkey TRIM5α cDNA was amplified by RT-PCR of mRNA extracted from rhesus monkey kidney LLC-MK2 cells using 5′-GCGGCCGCTACTATGGCTTCTGG-3′ as the forward primer and 5′-GAATTCTCAAGAGCTTGGTGA-3′ as the reverse primer. Amplified products were then cloned into the vector pCR-2.1TOPO (Invitrogen, Carlsbad, CA) and the nucleotide sequence authenticity was verified. For generating rhesus monkey TRIM5α cDNA carrying an HA tag (YPYDVPDYAA) at its C-terminus (Rh-TRIM5α-HA), cloned rhesus monkey TRIM5α cDNA in pCR-2.1TOPO was used as a template for PCR-amplification with a primer (5′-TCAAGCAGCATAATCAGGAACATCATAAGGATAAGAGCTTGGTGAGCACAGAG-3′) containing a nucleotide sequence corresponding to the HA-tag (underline) fused with the C-terminal portion of TRIM5α. The C-terminal portion of TRIM5α fused with the HA-tag (*Bam*HI to *Not*I) and the N-terminal portion of TRIM5α (*Not*I to *Bam*HI) was assembled on a pCEP4 vector (Invitrogen). Construction of cynomolgus monkey TRIM5α carrying an HA tag at the C-terminus (CM-TRIM5α-HA) was described previously (Nakayama et al., 2005).

To generate 121 chimeric TRIM5α, the 188-bp *Sph*I–*Bam*HI fragment of rhesus monkey TRIM5α was replaced with the corresponding 182-bp *Sph*I–*Bam*HI fragment of cynomolgus monkey TRIM5α in the background of Rh-TRIM5α-HA. Conversely, the 182-bp *Sph*I–*Bam*HI fragment of cynomolgus monkey TRIM5α was replaced with the 188-bp *Sph*I–*Bam*HI fragment of rhesus monkey TRIM5α in the background CM-TRIM5α-HA to generate 212 chimeric TRIM5α. To generate 112 chimeric TRIM5α, the C-terminal portion of CM-TRIM5α-HA (*Bam*HI to *Not*I) and the N-terminal portion of rhesus monkey TRIM5α were assembled on a pcDNA3.1 ( ) vector (Invitrogen). Conversely, the C-terminal portion of Rh-TRIM5α-HA (*Bam*HI to *Not*I) and the N-terminal portion of cynomolgus monkey TRIM5α (*Not*I to *Bam*HI) were assembled on a pcDNA3.1 ( ) vector to generate 221 chimeric TRIM5α. To generate 122 chimeric TRIM5α, the C-terminal portion of CM-TRIM5α-HA (*Sph*I to *Not*I) and the N-terminal portion of rhesus monkey TRIM5α (*Not*I to *Sph*I) were assembled on a pcDNA3.1 ( ) vector. Conversely, the C-terminal portion of Rh-TRIM5α-HA (*Sph*I to *Not*I) and the N-terminal portion of cynomolgus monkey TRIM5α (*Not*I to *Sph*I) were assembled on a pcDNA vector to generate 211 chimeric TRIM5α.

Mutant rhesus monkey TRIM5α lacking two amino acid residues TF at the 339th to 340th positions (Rh deltaTF TRIM5α), mutant rhesus monkey TRIM5α in which amino acid residues TFP at the 339th to 341st positions was replaced with a single amino acid Q found in cynomolgus monkey TRIM5α (Rh TFP-Q TRIM5α), and mutant cynomolgus monkey TRIM5α in which a single amino acid Q at the 339th position was replaced with three amino acid residues TFP found in rhesus monkey TRIM5α (CM Q-TFP TRIM5α) were generated by site-directed mutagenesis by PCR-mediated overlap primer exension method (Ho et al., 1989). Briefly, two DNA fragments with overlapping ends were generated by using the outer primers and the complementary primers with overlapping complementary nucleotides containing desired mutations. The resultant two fragments were combined in the subsequent fusion reaction in which the overlapping ends anneal, allowing the 3′ overlap of each strand to serve as a primer for 3′ extension of the complementary strand. The outer primers for generating Rh deltaTF

TRIM5α were 5′-GCGGCCGCTACTATGGCTTCTGG-3′ and 5′-GAATTCTCAAGAGCTTGGTGA-3′, and the complementary primers were 5′-GGGACATTATTTCCGTCACTCACG-3′ and 5′-CGTGAGTGACGGAAATAATGTCCC-3′. The outer primers were common in all cases of PCR-based mutagenesis of TRIM5α. The complementary primers for Rh TFP-Q TRIM5α were 5′-GGGACATTATTTCAATCACTCACG-3′ and 5′-CGTGAGTGATTGAAATAATGTCCC-3′ (underline; TFP-Q site), and 5′-GGACATTATTTACGTTTCCGTCACTCACG-3′ and 5′-CGTGAGTGACGGAAACGTAAATAATGTCC-3′ (underline; Q-TFP site) for CM Q-TFP TRIM5α.

2B2, 2S2, and 2P2 chimeric TRIM5α, which possessed the 188-bp *Sph*I–*Bam*HI fragment of baboon TRIM5α, 188-bp fragment of sooty mangabey TRIM5α, and 182-bp fragment of pig-tailed monkey TRIM5α, respectively, in the background of CM-TRIM5α-HA were generated by the same method as described above. To obtain *Sph*I–*Bam*HI fragments of baboon and sooty mangabey TRIM5αs, cloned rhesus monkey TRIM5α was used as a template for PCR-amplification with outer primers described above and complementary primers containing a nucleotide sequence corresponding to the 330th to 339th amino acid residues of baboon TRIM5α (5′-CAGATAACGTATCAGGCACCAGGGACATTATTTTCGTTTCCG-3′ and 5′-CGGAAACGAAAATAATGTCCCTGGTGCCTGATACGTTATCTG-3′) and the 334th to 343rd amino acid residues of sooty mangabey TRIM5α (5′-CAGGCACGAGGGACATTATTTTCGTTTCCGTCACACACGAAT-3′ and 5′-ATTCGTGTGTGACGGAAACGAAAATAATGTCCCTCGTGCCTG-3′), respectively. To obtain the *Sph*I–*Bam*HI fragment of pig-tailed TRIM5α, cloned cynomolgus monkey TRIM5α was used as a template for PCR-amplification with outer primers described above and complementary primers containing a nucleotide sequence corresponding to the 330th to 350th amino acid residues of pig-tailed monkey TRIM5α (5′-CAGTCACTCACGAATTTCATTTATTGTACTGGCATCCTGGGC-3′ and 5′-CGTGAGTGACTGAAATAATGTCCCTTGTGTCCGATACATTATCTG-3′). The entire coding sequences of those TRIM5α were then transferred to the *Not*I site of pSeV18+b(+). Recombinant SeVs carrying various TRIM5α were recovered according to a previously described method (Nakayama et al., 2005). The viruses passaged twice in embryonated chicken eggs were used as stock for all experiments.

### *Viral infection*

$2 \times 10^5$ MT4 or Hut78 cells were infected with SeV expressing each TRIM5α at a multiplicity of infection of 10 plaque-forming units per cell and incubated at 37 °C for 9 h. Cells were then superinfected with 20 ng of p24 of HIV-1 NL43, 20 ng of p27 of SIVmac239, or 20 ng of p25 of HIV-2 GH123, GH123/Q, or other HIV-2 isolates. The culture supernatants were collected periodically, and the level of p24, p27, or p25 was measured with a RETROtek antigen ELISA kit (ZeptoMetrix, Buffalo, NY).

### *Western blot analysis*

MT4 cells infected with recombinant SeVs expressing HA-tagged TRIM5α proteins were lysed in lysis buffer (50 mM Tris–HCl, pH 7.5, 150 mM NaCl, 1% Nonident P40, 0.5% sodium deoxycholate). TRIM5α proteins in the lysates were subjected to sodium dodecyl sulfate-polyacrylamide gel electrophoresis (SDS-PAGE). Proteins in the gel were then electronically transferred to a membrane (Immobilion; Millipore, Billerica, MA). Blots were blocked and probed with anti-HA high affinity rat monoclonal antibody (Roche, Indianapolis, IN) overnight at 4 °C. Blots were then incubated with peroxidase-conjugated anti-rat IgG (American Qualex, San Clemente, CA), and bound antibodies were visualized with a Chemilumi-One chemiluminescent kit (Nacalai Tesque, Kyoto, Japan).

### *TRIM5 cDNA sequences*

TRIM5α cDNA sequences for rhesus monkey (AY523632), cynomolgus monkey (AB210052), baboon (AY843505), sooty mangabey (AY10303), and pig-tailed monkey (AY899887–AY899893) were obtained from the GeneBank database.

## Acknowledgments

The authors would like to thank Setsuko Bandou and Noriko Teramoto for their assistance. HIV-2 UC2, UC12, and UC14 viruses were kind gifts from Jay A. Levy. This work was supported by grants from the Human Health Foundation, the Ministry of Education, Culture, Sports, Science, and Technology, and the Ministry of Health, Labor and Welfare, Japan.

## References

Anderson, J.L., Campbell, E.M., Wu, X., Vandegraaff, N., Engelman, A., Hope, T.J., 2006. Proteasome inhibition reveals that a functional preintegration complex intermediate can be generated during restriction by diverse TRIM5 proteins. J. Virol. 80, 9754–9760.

Barnett, S.W., Murthy, K.K., Herndier, B.G., Levy, J.A., 1994. An AIDS-like condition induced in baboons by HIV-2. Science 266, 642–646.

Berthoux, L., Sebastian, S., Sayah, D.M., Luban, J., 2005. Disruption of human TRIM5α antiviral activity by nonhuman primate orthologues. J. Virol. 79, 7883–7888.

Brennan, G., Kozyrev, Y., Kodama, T., Hu, S.L., 2007. Novel TRIM5 isoforms expressed by *Macaca nemestrina*. J. Virol. 81, 12210–12217.

Castro, B.A., Nepomuceno, M., Lerche, N.W., Eichberg, J.W., Levy, J.A., 1991. Persistent infection of baboons and rhesus monkeys with different strains of HIV-2. Virology 184, 219–226.

Diaz-Griffero, F., Li, X., Javanbakht, H., Song, B., Welikala, S., Stremlau, M., Sodroski, J., 2006. Rapid turnover and polyubiquitylation of the retroviral restriction factor TRIM5. Virology 349, 300–315.

Dormant, D., Livartowski, J., Chamaret, S., Guetard, D., Hein, D., Levagueresse, R., van de Moortelle, P.F., Larke, B., Gourmelon, P., Vazeux, R., Metivier, H., Flageat, J., Court, L., Hauw, J.J., Montagnier, L., 1989. HIV-2 in rhesus monkeys: serological, virological and clinical results. Intervirology 30, 59–65.

Franchini, G., Fargnoli, K.A., Giombini, F., Jagodzinski, L., De Rossi, A., Bosch, M., Biberfeld, G., Fenyo, E.M., Albert, J., Gallo, R.C., Wong-Staal, F., 1989. Molecular and biological characterization of a replication competent human immunodeficiency type 2 (HIV-2) proviral clone. Proc. Natl. Acad. Sci. U. S. A. 86, 2433–2437.

Franchini, G., Markham, P., Gard, E., Fargnoli, K., Keubaruwa, S., Jagodzinski, L., Robert-Guroff, M., Lusso, P., Ford, G., Wong-Staal, F., Gallo, R.C., 1990. Persistent infection of rhesus macaques with a molecular clone of human immunodeficiency virus type 2: evidence of minimal genetic drift and low pathogenetic effects. J. Virol. 64, 4462–4467.

Hahn, B.H., Shaw, G.M., De Cock, K.M., Sharp, P.M., 2000. AIDS as a zoonosis: scientific and public health implications. Science 287, 607–614.

Hatziioannou, T., Perez-Caballero, D., Yang, A., Cowan, S., Bieniasz, P.D., 2004. Retrovirus resistance factors Ref1 and Lv1 are species-specific variants of TRIM5α. Proc. Natl. Acad. Sci. U. S. A. 101, 10774–10779.

Ho, S.N., Hunt, H.D., Horton, R.M., Pullen, J.K., Pease, L.R., 1989. Site-directed mutagenesis by overlap extension using the polymerase chain reaction. Gene 77, 51–59.

Kaiser, S.M., Malik, H.S., Emerman, M., 2007. Restriction of an extinct retrovirus by the human TRIM5α antiviral protein. Science 316, 1756–1758.

Keckesova, Z., Ylinen, L.M., Towers, G.J., 2004. The human and African green monkey TRIM5α genes encode Ref1 and Lv1 retroviral restriction factor activities. Proc. Natl. Acad. Sci. U. S. A. 101, 10780–10785.

Locher, C.P., Barnett, S.W., Herndier, B.G., Blackbourn, D.J., Reyes-Teran, G., Murthy, K.K., Brasky, K.M., Hubbard, G.B., Reinhart, T.A., Haase, A.T., Levy, J.A., 1998. Human immunodeficiency virus-2 infection in baboons is an animal model for human immunodeficiency virus pathogenesis in humans. Arch. Pathol. Lab. Med. 122, 523–533.

Locher, C.P., Witt, S.A., Herndier, B.G., Tenner-Racz, K., Racz, P., Levy, J.A., 2001. Baboons as an animal model for human immunodeficiency virus pathogenesis and vaccine development. Immunol. Rev. 183, 127–140.

McClure, J., Schmidt, A.M., Rey-Cuille, M.A., Bannink, J., Misher, L., Tsai, C.C., Anderson, D.M., Morton, W.R., Hu, S.L., 2000. Derivation and characterization of a highly pathogenic isolate of human immunodeficiency virus type 2 that causes rapid CD4+ cell depletion in *Macaca nemestrina*. J. Med. Primatol. 29, 114–126.

Nakayama, E.E., Miyoshi, H., Nagai, Y., Shioda, T., 2005. A specific region of 37 amino acid residues in the SPRY (B30.2) domain of African green monkey TRIM5α determines species-specific restriction of simian immunodeficiency virus SIVmac infection. J. Virol. 79, 8870–8877.

Nakayama, E.E., Maegawa, H., Shioda, T., 2006. A dominant-negative effect of cynomolgus monkey tripartite motif protein TRIM5α on anti-simian immunodeficiency virus SIVmac activity of an African green monkey orthologue. Virology 350, 158–163.

Newman, R.M., Hall, L., Connole, M., Chen, G.L., Sato, S., Yuste, E., Diehl, W., Hunter, E., Kaur, A., Miller, G.M., Johnson, W.E., 2006. Balancing selection and the evolution of functional polymorphism in Old World monkey TRIM5α. Proc. Natl. Acad. Sci. U. S. A. 103, 19134–19139.

Nicol, I., Flamminio-Zola, G., Doubouch, P., Bernard, J., Snart, R., Jouffre, R., Reveil, B., Fouchard, M., Desportes, I., Nara, P., Gallo, R.C., Zagury, D., 1989. Persistent HIV-2 infection of rhesus macaque, baboon, and mangabeys. Intervirology 30, 258–267.

Ohkura, S., Yap, M.W., Sheldon, T., Stoye, J.P., 2006. All three variable regions of the TRIM5α B30.2 domain can contribute to the specificity of retrovirus restriction. J. Virol. 80, 8554–8565.

Perez-Caballero, D., Hatziioannou, T., Yang, A., Cowan, S., Bieniasz, P.D., 2005. Human tripartite motif 5α domains responsible for retrovirus restriction activity and specificity. J. Virol. 79, 8969–8978.

Perron, M.J., Stremlau, M., Song, B., Ulm, W., Mulligan, R.C., Sodroski, J., 2004. TRIM5α mediates the postentry block to N-tropic murine leukemia viruses in human cells. Proc. Natl. Acad. Sci. U. S. A. 101, 11827–11832.

Reymond, A., Meroni, G., Fantozzi, A., Merla, G., Cairo, S., Luzi, L., Riganelli, D., Zanaria, E., Messali, S., Cainarca, S., Guffanti, A., Minucci, S., Pelicci, P.G., Ballabio, A., 2001. The tripartite motif family identifies cell compartments. EMBO J. 20, 2140–2151.

Sawyer, S.L., Wu, L.I., Emerman, M., Malik, H.S., 2005. Positive selection of primate TRIM5α identifies a critical species-specific retroviral restriction domain. Proc. Natl. Acad. Sci. U. S. A. 102, 2832–2837.

Song, B., Gold, B., O'Huigin, C., Javanbakht, H., Li, X., Stremlau, M., Winkler, C., Dean, M., Sodroski, J., 2005a. The B30.2(SPRY) domain of the retroviral restriction factor TRIM5α exhibits lineage-specific length and sequence variation in primates. J. Virol. 79, 6111–6121.

Song, B., Javanbakht, H., Perron, M., Park, D.H., Stremlau, M., Sodroski, J., 2005b. Retrovirus restriction by TRIM5α variants from Old World and New World primates. J. Virol. 79, 3930–3937.

Song, H., Nakayama, E.E., Yokoyama, M., Sato, H., Levy, J.A., Shioda, T., 2007. A single amino acid of the human immunodeficiency virus type 2 capsid affects its replication in the presence of cynomolgus monkey and human TRIM5αs. J. Virol. 81, 7280–7285.

Stremlau, M., Owens, C.M., Perron, M.J., Kiessling, M., Autissier, P., Sodroski, J., 2004. The cytoplasmic body component TRIM5α restricts HIV-1 infection in Old World monkeys. Nature 427, 848–853.

Stremlau, M., Perron, M., Welikala, S., Sodroski, J., 2005. Species-specific variation in the B30.2(SPRY) domain of TRIM5α determines the potency of human immunodeficiency virus restriction. J. Virol. 79, 3139–3145.

Stremlau, M., Perron, M., Lee, M., Li, Y., Song, B., Javanbakht, H., Diaz-Griffero, F., Anderson, D.J., Sundquist, W.I., Sodroski, J., 2006. Specific recognition and accelerated uncoating of retroviral capsids by the TRIM5α restriction factor. Proc. Natl. Acad. Sci. U. S. A. 103, 5514–5519.

Wu, X., Anderson, J.L., Campbell, E.M., Joseph, A.M., Hope, T.J., 2006. Proteasome inhibitors uncouple rhesus TRIM5α restriction of HIV-1 reverse transcription and infection. Proc. Natl. Acad. Sci. U. S. A. 103, 7465–7470.

Yap, M.W., Nisole, S., Lynch, C., Stoye, J.P., 2004. Trim5α protein restricts both HIV-1 and murine leukemia virus. Proc. Natl. Acad. Sci. U. S. A. 101, 10786–10791.

Yap, M.W., Nisole, S., Stoye, J.P., 2005. A single amino acid change in the SPRY domain of human Trim5α leads to HIV-1 restriction. Curr. Biol. 15, 73–78.

Ylinen, L.M., Keckesova, Z., Wilson, S.J., Ranasinghe, S., Towers, G.J., 2005. Differential restriction of human immunodeficiency virus type 2 and simian immunodeficiency virus SIVmac by TRIM5α alleles. J. Virol. 79, 11580–11587.